



UNIVERSITY OF OXFORD

THIRD YEAR PROJECT

Detecting sleep apnoea via non-invasive methods

Authors:

George COCHRANE

Sophie LOUTH

Tuan Anh LE

Sachin MYLAVARAPU

Supervisor:

Dr. Frank PAYNE

April 26, 2014

Abstract

The abstract text goes here.

Contents

1	Introduction	3
2	Medical Information	4
3	Rationale	6
3.1	Medical Need	6
3.1.1	Prevalence	7
3.1.2	Long Term Effects	8
3.2	Economic Rationale	9
3.2.1	Current Solutions	9
3.2.2	Proposed App - Where it fits in	12
3.2.3	Advantages of proposed app	12
4	The app	15
5	Design Process	16
5.1	Diagnostic Methods	16
5.2	Signs and Symptoms – non-invasive methods	17
5.2.1	Video	18
5.2.2	Accelerometry	19
5.2.3	Audio	19
5.2.4	Questionnaire	19
5.2.5	Conclusion	19
5.3	Questionnaire selection	20
5.3.1	Own vs Pre-Existing	20

5.3.2	How Truthful are People	20
5.3.3	Questionnaires	21
5.3.4	Narrowing Down the Studies	22
5.4	Audio	22
5.4.1	Scoring of apnea R&K vs AASM	22
5.4.2	Methods of Analysis	23
5.5	Signal Analysis – simple method	30
5.5.1	Outline	30
5.5.2	Implementation in MATLAB [®]	31
5.5.3	Limitations of model	36
5.6	Machine Learning – Theory	37
5.6.1	Support Vector Machines	38
5.6.2	State-Space Models	42
5.6.3	Hidden Markov Models	44
5.6.4	Conditioning input data	49
5.7	Machine Learning – Experiments	53
5.7.1	Conditioning input data	54
5.7.2	Data Visualisation	55
5.7.3	Support Vector Machines	56
5.7.4	Hidden Markov Models	58
5.7.5	Summary	64
5.8	Machine Learning – Java	66
5.9	Android	67
6	Conclusion	68

Chapter 1

Introduction

Lorem ipsum dolor sit amet, consectetur adipisicing elit, sed do eiusmod tempor incididunt ut labore et dolore magna aliqua. Ut enim ad minim veniam, quis nostrud exercitation ullamco laboris nisi ut aliquip ex ea commodo consequat. Duis aute irure dolor in reprehenderit in voluptate velit esse cillum dolore eu fugiat nulla pariatur. Excepteur sint occaecat cupidatat non proident, sunt in culpa qui officia deserunt mollit anim id est laborum.

Chapter 2

Medical Information

Obstructive Sleep Apnea (OSA), sometimes called hypersomnia sleep apnea syndrome, occlusive sleep apnea, sleep disordered breathing, hyperventilation syndrome and Pickwickian Syndrome, however the latter three are discouraged because they are also used to describe other disorders, is a sleep disorder characterised by repetitive blockages in the upper airway during sleep, but with inspirational effort. These blockages can be apneas, full closure, or hypopneas, partial closure, both cause a restriction in airflow, which can lead to reduction in oxygen saturation and frequent arousal in order to re-establish airflow.

The upper airways include the nasal cavity, oral cavity and pharynx, the area behind the tongue, the main part that becomes blocked is the pharynx, this is usually held open by the pharyngeal dilator muscles, although these relax during sleep, in a healthy subject they are still able to maintain airflow, however in an OSA sufferer they provide insufficient force to prevent collapse. Collapse occurs during inspiration only due to negative pharyngeal pressure. During rapid eye movement (REM) sleep there is further relaxation of the pharyngeal dilator muscle manifesting as a decrease in tone and activity which can lead to longer apnea and hypopnea events.

Many factors affect the likelihood a patient suffers with OSA, however one thing is consistent in almost all cases; the pharyngeal upper airway size is smaller than in normal patients and often more elliptical, this can have a number of causes including fat deposits and facial bone structure. Overweight and obese patients often have fat deposits lateral to the pharynx, not always substantial but its positioning creates or reinforces elliptical shape and reduction in size. The main element of facial bone structure that influence upper airway size is the positioning of the maxilla and mandible (upper and lower jaw bones), these can influence the airway size in a number of ways, retrognathia where the mandible is smaller and therefore

appears to be set back or both jaw bones can be the same size but set back in both of these cases the tongue sits further back in the mouth, increasing tendency to block airflow. Lower positioning of the hyoid bone and Brachycephaly where the head is wider than it is tall can have a similar effect.

Abnormal facial tissues can also have an effect, large tonsils and adenoids, elongated or enlarged uvula (the dangly bit at the back of the mouth), macroglossia (enlarged tongue), high arched or narrow hard palate, reduced nasal patency (cross sectional area) possibly caused by nasal abnormalities all have been shown to factor.

Other factors include lying supine (on back) which allows gravity to pull the tongue into the airway. Some drugs including alcohol relax the pharyngeal dilator muscles more than just the effects of sleep, worsening OSA. Smoke irritates tissues including those in the upper airways, swelling them such that they cause a narrowing of the airway.

Chapter 3

Rationale

3.1 Medical Need

Medical need can essentially be split down into two areas: prevalence i.e. how many people suffer; and consequences, what people will die of and what their quality of life will be. There are a few other things that hint at the medical need and others opinions of that.

The British Lung Foundation has prioritised OSA and created an OSA Charter calling on the UK governments to make OSA a national priority as well as encouraging investment in research. They held a three year campaign to raise awareness which ended in 2014 The campaign had two aims: to increase awareness both to the general public and health care professionals and to improve diagnosis. Part of the plan to improve diagnosis was to develop a national standard for diagnosis that would include a one stop shop so that the patient pathway would be reduced in length in order to reduce concerns about driving. A conference on OSA was held in February 2014 where doctors expressed desire to change the current system, due to increased need for doctor referral of patients to sleep centres.

PhysioNet and Computers in Cardiology with funding from Margret and H.A. Rey Laboratory for Nonlinear Dynamics in Medicine set up a competition with two prizes of \$500 for whoever could classify ECG data, obtained minimally intrusively and inexpensively, into that from OSA sufferers and normal subjects, with the intension of using it as a screening tool.

The Agency for Healthcare Research and Quality (AHRQ) felt that the diagnosis of sleep apnea was a sufficiently important public health issue that they commissioned a study on future research needs which includes a reference to the need for portable monitors, including limited-channel, low-cost portable devices.

3.1.1 Prevalence

Prevalence of OSA is hard to know due to the fact a high levels of cases go undiagnosed, however estimates range from 1 to 28% depending on severity and location.

There may be an ethnicity element in prevalence, however few studies have been undertaken other than in western countries and therefore prevalence elsewhere is essentially unknown. However for some areas it is known, this means study on causes can be undertaken for example prevalence in Western Nations and Hong Kong is very similar however prevalence of risk factors is very different, there are high levels of obesity in the west but not in those studied from Hong Kong, so hypotheses have been produced on other risk factors including facial features being more prevalent in Hong Kong and some clinical observations support these.

Gender has been shown to have an effect with estimates of 2 to 3 times great risk for men compared to women. However the reasons behind this are unclear. Hormones have been considered but administration of the female hormones oestrogen and progesterone to men does not appear to have an effect. Men show greater prevalences to many chronic diseases so this may be part of a greater trend and differences elsewhere have been shown to be linked to physical features, occupation, environment, attitude to health and risky behaviour. There are gender differences in upper airway shape, muscle activity, facial shape, and deposition of fat in the airway, however the few studies that have looked at this have yet to find a conclusive link. Whereas occupation, attitude to health and risky behaviour have not been studied while specifically looking at gender disparity in OSA.

There are hypotheses proposing higher prevalence of OSA in pregnant mothers however few data to support this. Proposed mechanisms to cause this include excess weight gain and the effect of sleep deprivation on pharyngeal dilator muscle activity.

Although a positive trend between OSA prevalence and age appears to exist for mid life the same isnt true for younger or older patients. OSA in children has similar consequence to that in adults and some of the pathophysiology (physical manifestation of a disease) is the same, however the etiology (causes) and associated morbidity (rate of incidence of a disease) can be very different, which means that it is generally studied independently from the adult form.

In old age prevalence of OSA increases however this doesnt necessarily mean that physiological changes associated with old age are causing OSA. If this was the case one would expect the prevalence rate to increase at the same rate as through middle age or at a higher rate. Figure X shows the Sleep Heart Health

Study on prevalence with age which starts to flatten in the 60s which suggests age related prevalence tails off at this point.

It is possible that older age OSA is actually distinct from that of middle age, several studies support this theory, as many of the key symptoms of middle age OSA are not present in the old age version including, daytime sleepiness, obesity, decrease in cognitive function and hypertension. Snoring is also significantly less reported however this could be caused by increase in bed partner hearing loss and death.

3.1.2 Long Term Effects

There is an association between OSA and secondary hypertension (high blood pressure) independent of excess weight and other factors. This link is seen even in mild OSA, and given the prevalence of OSA could be having an impact on a significant proportion of those suffering with hypertension. However attempts to treat OSA in order to reduce hypertension have so far yielded unclear results.

Hypertension is linked to cardiovascular and cerebrovascular disease and therefore given the link between OSA and hypertension, OSA will moderately contribute to the morbidity and mortality of these. There may also be direct links between OSA and cardiovascular disease however this has been less well studied. Whether treatment of OSA can improve cardiovascular disease has yet to be assessed.

Daytime sleepiness is a primary feature of OSA and many studies have shown that treatment of OSA does reduce daytime sleepiness. Studies have found a significant association between snoring and daytime sleepiness. Snoring is a strong indicator of OSA, so the link between OSA and daytime sleepiness could be due to snoring, studies have shown the association between snoring and daytime sleepiness is independent of OSA.

The effects of OSA on cognitive function is not fully understood, there are some population based studies which find weaker correlations than clinic based studies, this is probably due to the biased population who attend sleep laboratories. In one study OSA was significantly but weakly related to reduced psychomotor efficiency (a measure of coordination of fine motor control with sustained attention), this link was not explained by daytime sleepiness. In another study of self reported snorers a weak but significant association was found between OSA and neuropsychological function.

There is a thought that during OSA the restricted airflow causes a reduction in oxygen supply to the brain which in turn causes changes in the neurons of the hippocampus and the right frontal cortex. This atrophy has been shown using neuro-imaging to be irreversible even with CPAP and is seen in 25% of OSA cases. The effects are problems with mentally manipulating non-verbal information, and in working

memory and executive functions.

There is no specific quality of life measure for OSA although one is being developed, however the SF-36 a general health-related quality of life measure, a short form of the Medical Outcomes Study, is in use. A couple of studies have found a linear association between severity of OSA and decrements on the SF-36 scales, showing undiagnosed OSA has a similar affect on quality of life to other chronic disorders of similar severity, although another study showed a threshold effect as severity of OSA increased on a study of self-reported sleepiness or snoring, however a small sample size limits usability.

Patients with OSA have a higher vehicle crash rate than the general populous, this has been shown by crash records, self-reports and performance on driving simulators. This is a significant issue because it puts the lives of everyone not just the sufferers at risk. Studies undertaken in clinic will over estimate rate of crashes due to selection bias, however there are population studies looking at those with undiagnosed OSA which also show a strong correlation, especially among men. Self-reported sleepiness was not able to explain the crash rate. This is concerning because it means those at risk are not able to recognise it within themselves and are therefore unable to take precautions to reduce risk.

3.2 Economic Rationale

3.2.1 Current Solutions

As is evident, sleep apnea, particularly obstructive sleep apnea (OSA) affects a significant proportion of the population and is worthy of attention. The current available diagnosis options for sufferers or potential sufferers are limited, expensive, invasive and relatively inaccessible. We outline below the most common sources of help and diagnosis for potential sufferers:

- NHS - GP check-up, home devices and polysomnography (PSG)
- Commercial home-testing devices
- Other possible future options such as mobile sleep apps and non-contact health sensing technologies

NHS

According to the NHS guidelines, patients who believe they may be suffering from sleep apnea can schedule a visit to their GP. The GP will ask a few questions to determine the likelihood of apnea, along with a physical examination that includes a blood pressure (BP) test and a hypothyroidism test, to determine whether an underactive thyroid gland is the reason for the patient's tiredness. The patient can then choose

if he/she would like to be observed for one night in a sleep centre, or would like to be given a monitoring device to wear at home when sleeping. Those who opt for a home sleep study are required to visit the sleep centre at a convenient time to collect and learn how to use the portable recording equipment. These include breathing sensors, heart rate monitors and oxygen sensors. Information from the device can be analysed on the next visit and further action, such as referring to a sleep centre can be taken [9, 10].

Observation at a sleep centre is done through polysomnography (PSG). This involves electrodes being placed on the face, scalp and above the lips, and bands being placed around the chest and abdomen. Additionally, sensors are placed on the legs and an oxygen sensor is attached to a finger. The tests carried out during a PSG include:

- Electro-encephalography (EEG)
- Electromyography (EMG)
- Recording of thoracoabdominal movements
- Recording of oronasal airflow
- Pulse Oximetry
- Electrocardiography (ECG)
- Sound and Video Recording

The data from these tests is used to positively diagnose obstructive sleep apnea and a treatment regimen is then decided upon and enforced by the healthcare professional [9]. For the purposes of this report, we shall not delve into the treatment of OSA - we concern ourselves with the diagnosis process and how we can improve it.

Commercial home-testing devices

While these devices are more common in the United States, they are also available in the UK, and can be purchased if desired without visiting a GP. An example of such home-testing devices is the AccuSom[®] test from NovaSom Inc. [11, 12], pictured below:

The prevalence of such tests in the U.S. points towards the increasing unfeasibility of sleep centre tests for simple diagnosis of OSA, and is an indication of where the diagnosis process is headed in the future, in the U.K. as well as around the world. The economic reasons for the trend are clear. On average, a single night at a sleep centre and the associated tests could cost from \$800 to \$3000 in the U.S [4]. (figures for the NHS in the U.K. are more difficult to find, but should be comparable) The home tests can be



Figure 3.1: AccuSom® [12]

administered at a fraction of that price, ranging from \$200 to \$600 [4]. Moreover, sleep centre tests are extremely inconvenient for the patients, and hence should be administered towards the later stages of the diagnosis process. The use of home-testing devices also allows a larger percentage of the population to be able to test for OSA, which is desirable given that around 5% suffer from undiagnosed OSA [10].

Other options

The trend towards greater user independence in OSA diagnosis is further observed through two major related breakthroughs - the rise of mobile sleep apps and the development of non-contact health sensing technologies.

The popularity of sleep monitoring apps in the iOS and Android App stores illustrates an increasing interest among smartphone users in their sleep patterns. Currently, such apps use the accelerometers and microphones to detect movements and noises from the users while they sleep, and use relatively simple algorithms to determine which stage of sleep the user is in. In addition, some apps come with additional headsets or headbands that track electrical impulses and measure the user's activity more accurately. The alarm clock function is activated only when the user is in light sleep (within a reasonable time window) to ensure he/she is woken up feeling energised [13]. Some examples of such apps are:

- Sleep Cycle (iOS) - \$1
- Sleep Bot Tracker (Android) - Free
- Wakemate - \$60
- Lark - \$99

- Zeo Sleep Manager Mobile - \$99
- Sleep Tracker Elite - \$149

The development of non-contact health sensing technologies holds promise as well. Recently, Xerox and Manipal University Hospital in India announced a collaboration to develop such technologies at Xerox's research centre in Bangalore [17, 6]. Using image and signal processing algorithms, the collaboration aims to determine health indicators in a non-invasive manner, and such that monitoring can take place remotely [17]. The clear trend of health monitoring towards non-invasive methods and the increasing use of algorithms to supplement health care and diagnosis efforts is set to gain even more momentum as healthcare professionals begin to embrace 'big data' [14].

3.2.2 Proposed App - Where it fits in

The need for an app that is able to diagnose OSA from a mobile platform, using non-invasive techniques is clear from the current diagnosis solutions and trends. While there has been a shift towards cheaper home-testing devices before necessitating a visit to a sleep centre, the fact remains that even at \$200, these tests are not inexpensive. What if we could create a means for diagnosing OSA without the need for cumbersome and invasive sensors, that could be accessed by anyone with a smartphone, at a negligible cost compared to a home-testing system? Those who have doubts over their sleep habits, but are too busy for a GP visit and do not want to spend money unnecessarily on a home-testing system, could try the app and move on to pursue the matter more seriously - if the results from the app suggested a need to do so. Since machine learning algorithms will be used in the processing of the data, the app has the potential to continuously improve in accuracy and, eventually, could outperform the home-testing devices. The development of image processing technology that could remove the need for invasive monitoring, especially in neonatal care, by Manipal University Hospital and Xerox sets a precedent and raises the possibility of diagnosing OSA without the need for sensors being placed around the body.

3.2.3 Advantages of proposed app

The advantages of the proposed smartphone app, that will use machine learning algorithms to accurately diagnose OSA using non-invasive mobile phone sensors, are numerous. Firstly, such an app, if utilised as a precursor to home-testing systems and sleep centres, could result in significant cost savings for both the healthcare provider and the patient. From the point of view of the NHS, savings from performing polysomnograms only on those who really need it would be substantial. Moreover, some of the functions

such as collecting information about the patient can be done through the app using questionnaires to save time for the doctors. From the point of view of the patients, not having to schedule visits to the GP for collecting and returning home-testing kits would result in a larger number of users for the app than would otherwise have been the case. This brings us to another advantage of using the mobile app - accessibility. Given that 65 % of people over 65 in the U.K. have OSA [10], along with a significant proportion of middle-aged men and women, and that the condition often goes undiagnosed, it is essential to reach out to as many users as possible. The best way to do so is through mobile phones. The number of smartphone users is projected to increase globally from 1.75 billion in 2014 to almost 2.5 billion by 2017 [1]. The graph below highlights the growth of mobile phone users worldwide:

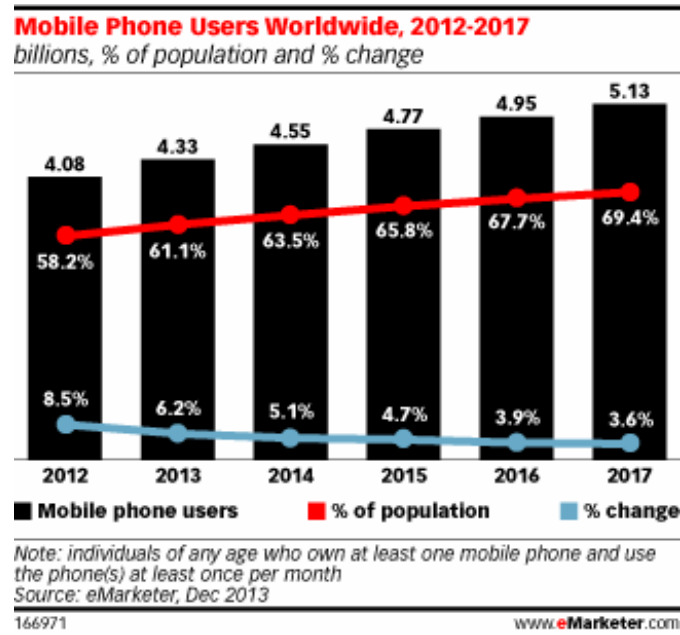


Figure 3.2: Mobile Phone Users 2012 - 2017 [1]

This highlights the potential for the app, and smartphone-aided diagnosis in general, not just in the U.K. but in other developing countries as well, where access to a sleep centre may not be as readily available.

The advantage that the proposed app holds over existing mobile phone apps is that it is specifically for diagnosing OSA - it is meant for medical purposes as opposed to general sleep cycle monitoring. This means that it does not compete with the above-mentioned apps, but serves a distinct purpose which is not possible in the other apps. Moreover, the use of machine learning algorithms in the app means that there is potential for the app to improve in accuracy over time as the amount and quality of training data used is improved. With every update, the app can become better at diagnosing OSA using only

non-invasive methods.

In conclusion, the rationale for the project to develop such an app is clear. If developed, the app is viable as a supplementary service by the NHS and can improve the diagnosis of OSA in adults in the U.K. dramatically by reaching out to a wider audience and simultaneously result in savings for the NHS. It can also be further developed for use internationally, by those in developing countries in the future.

Chapter 4

The app

Lorem ipsum dolor sit amet, consectetur adipisicing elit, sed do eiusmod tempor incididunt ut labore et dolore magna aliqua. Ut enim ad minim veniam, quis nostrud exercitation ullamco laboris nisi ut aliquip ex ea commodo consequat. Duis aute irure dolor in reprehenderit in voluptate velit esse cillum dolore eu fugiat nulla pariatur. Excepteur sint occaecat cupidatat non proident, sunt in culpa qui officia deserunt mollit anim id est laborum.

Chapter 5

Design Process

5.1 Diagnostic Methods

There are four strategies used to approach diagnosis they are; the algorithmic method, pattern recognition method, hypothetico-deductive method; sometimes called differential diagnosis, and the exhaustive method.

The algorithmic method uses flowcharts and algorithms to analyse data that are precise and reproducible for example vitamin B12 level in blood. One follows steps making decisions at preselected branch point based on the clinical data available. This relies on a flow chart for the illness and the illness to present in a relatively normal way. Abnormal presentation of an illness could easily lead to misdiagnosis. For example if an OSA sufferer is not overweight but instead has lateral peritonsillar narrowing, they may well be missed by this method.

The pattern recognition method, is best for conditions with distinct presentation, especially those which present regularly in the population. It is referred to as pattern recognition because the symptoms and signs displayed by the patient reawakens memories in the doctor of previous examples. It is an efficient method, especially useful when time critical diagnoses are needed. This does however risk jumping prematurely to a final hypothesis, although the consequences of this can be reduced by follow up in order to check instincts.

The hypothetico-deductive method lends itself to primary care settings as it results in a differential diagnosis, a rank ordered list of hypotheses. Hypotheses are generated and rejected as more data are collected and questions asked until a working hypothesis is reached. This method is most often used as it reflects how most people deal with life, and is therefore the most natural. It can cause errors if a doctor has

been exposed to a certain diagnosis recently, they may choose to ignore signs that what they are looking at is in fact not that. For example if a doctor has diagnosed and number of patients with OSA recently (or read a paper about it) they may diagnose a patient who expresses day time sleepiness and witnessed apneas with OSA when in fact the previous traumatic head injury would be an indicator for Central Sleep Apnea, in this case a polysomnogram would be needed to see whether the patient was actually attempting respiration during apneas. Another error situation can be caused by the doctor failing to think about the probability of a diagnosis being correct. for example, if a patient presents with witnessed choking during sleep as the primary symptom rather than daytime sleepiness or witnessed apneas the doctor may diagnose Sleep Choking Syndrome however this has a much lower prevalence than OSA, rare compared to about 2-4% for OSA.

The exhaustive method works on the premise of having all the information, all data collected, all questions asked. Completeness of data is important for hospitalised patients but acquiring it is too time consuming and expensive for most cases. Useful for unusual illness when other methods have failed or for unusual expressions of illnesses.

The hypothetico-deductive method will be useful in order to establish what symptoms and signs can be used to differentiate OSA from other disorders. However the app itself will need to rely on pattern recognition because ruling out all options will be impossible as a doctor wont be administering the app. It was also be unnecessary to use an exhaustive method as the app is only designed to pick up OSA not all sleep disorders or reasons for daytime tiredness.

5.2 Signs and Symptoms – non-invasive methods

Table X shows all the known signs and symptoms of OSA along with detectable presentation. From there Table X+1 shows these presentations and the different sensors for measuring them, as well as whether those sensors are invasive or not. The non-invasive sensors shall be the focus of the following work. The presenting symptom for OSA is daytime sleepiness, with reports of snoring and witnessed apneas from the patients bed partner. So focussing on other conditions with these symptoms is a start to finding a unique combination of symptoms for OSA that can be tested non-invasively by an app.

Table X+2 looks at four key symptoms of OSA which the majority of patients display (and can be detected non-invasively). Disorders which also display one or more of these symptoms are then listed along with their differentiator from OSA. From the table it is clear most of these conditions can be ruled

out by diagnosis focussing on daytime sleepiness, snoring, and an apnea awakening/choking combination.

Ascertaining these would eliminate all but central sleep apnea and altitude insomnia however both of these would be picked up a significant proportion of the time by a questionnaire because the sufferers would only fit the risk cases for OSA in a small percentage of cases. Especially for altitude insomnia as those with a BMI over 35kgm⁻² are unlikely to be climbing over 4000m in height for extended periods (i.e. climbing mountains rather than flying).

Those suffering from central sleep apnea are likely to reflect population distribution for BMI as weight is not a cause or exacerbating factor. I.e. about 25% of central sleep apnea patients are obese (BMI > 30) compared to 70% of OSA sufferers.

Methods are then needed to detect daytime sleepiness, loud snoring and apnea arousal (choking) combinations. Sensors to look at are; video, accelerometry, audio and questionnaires. Idea and their merits and weaknesses will be discussed next.

5.2.1 Video

The aim is to pick up on apneas via cessation of breathing and arousal via significant body movement. Snoring would not be possible to detect although some other attributes that hint at OSA may be detectable e.g. lying in the supine position (on back). Video could also be used to detect sleep and activity, e.g. sleep cycle transitions and limb movements.

Merits include, smartphone already have cameras so an external camera wouldnt be needed, although the cameras may struggle with the low light level in the sleeping space, and changing the light level in order to accommodate the camera could have a knock on effect on the quality or type of sleep.

Weaknesses include, positioning of the camera will be important and this is hard when all rooms are different and smartphones dont naturally stand up by themselves. Manual analysis of the video has been used until recently so there isnt a great deal of statistical data on how well computer algorithms can detect OSA. Video produces large data files that cannot be sensibly stored on a phone. Video has formed part of the polysomnogram in some areas for a long time as an aide to observation and only recently investigated as an independent method of diagnosis using automated analysis. As a consequence lots of video data does exist however it is highly regulated due to patient confidentiality.

5.2.2 Accelerometry

This has the potential to be able to detect body position and sleep wake segmentation which could give a pretty good indicator of apnea arousal events, however mechanism for detecting snoring.

This has not been part of the polysomnogram although it has started to be investigated as a mechanism for detecting OSA. There is very little data available which makes a retrospective study a challenge, especially as there is no data combined with polysomnogram data for verification. Positioning of the phone in order to get the best results without damaging the phone would require some investigation. Non standardised arrangements of mattress and bed clothes may cause issues.

5.2.3 Audio

The most obvious way to detect audio signals from the patient is via the phones in built microphone although external microphones should also be investigated. It ought to be possible to detect apnea arousal events and snoring.

Lots of work has been done on audio analysis of speech so there are lots of ideas out there to work from. Many polysomnograms include a sound recording for reference so there is a lot of data available and in the most part it is anonymised so there isnt a risk to patient confidentiality. In some cases it has been labelled so it can be used easily for a retrospective study such as this one. There are also regulations which can act as a guideline.

5.2.4 Questionnaire

A questionnaire is pretty much the only way to assess daytime sleepiness, it can also be used to acquire about other symptoms and co-morbidities. If a preexisting questionnaire is used then there will be data on its effectiveness and usability and statistics it has produced. Questions for part of the diagnostic pathway so it takes some of the work away from the doctor. Some studies show patients are more truthful with anonymous questionnaires than with their doctor, more on that to follow.

5.2.5 Conclusion

Given that audio analysis and questionnaires should be sufficient to diagnose OSA and rule out other similar disorders, these will be investigated further with the other methods discarded unless significant issues are encountered with audio and questionnaire analysis.

5.3 Questionnaire selection

The key point that needs to be established via the questionnaire is whether the patient suffers from daytime sleepiness however knowing about the patients weight can be useful to eliminate central sleep apnea, and other questions about symptoms can be useful to reinforce diagnosis.

5.3.1 Own vs Pre-Existing

There is a key decision between two options at this stage, to create a new questionnaire from scratch or to use a pre-existing questionnaire. A new questionnaire gives much more freedom as to what questions to ask in order to target particular symptoms and eliminate other disorders. It also allows for unique methods of analysis e.g. weighted questions rather than a simple threshold based on number of questions answered. Rigorous market research can be used to design the wording of the questions to maximise truthfulness and ease of interpretation, as well as number of questions and mechanism of answering. However this would be time consuming and an expert in question production is potentially needed. Data from patients would need to be collected via the questionnaire and other means in order to test its effectiveness. Using pre-existing questionnaire allows for quicker set up time as there will either be data available in order to validate the questionnaire or it will have already been validated. Some questionnaires are within the doctors guideline so time can be saved during consultation if they are already performed. Named questionnaires are often recognised by doctors which saves them time checking the questions and they are also more likely to trust questionnaire they know. Given the time constraints and the access to data and skills further investigation will look at pre-existing questionnaires.

5.3.2 How Truthful are People

One of the benefits of performing questionnaires on the app rather than waiting for patients to attend an appointment is saving doctors time however there is another benefit in the form of increasing truthfulness. One study found that patients tended to lie in order to look good, in the context of sexuality, those involved had a strong interest in not giving a disappointing impression. Another study looked at doctors trust in patients which is an indicator of suspected lying. Ulterior motives were thought to have a significant influence on patients truthfulness. In the case of OSA there is a risk of patients playing down daytime sleepiness in order to avoid diagnosis if they wish to avoid having to contact the DVLA and their car insurance company and risk losing their license or insurance due to misunderstanding. There is also a

case that patients may try and get a diagnosis in order to receive disability related financial support, however tricking a night time study into thinking you have OSA would be challenging.

5.3.3 Questionnaires

There are a number of questionnaires that have been used to assess diagnosis of OSA, some rely on a doctor to measure physical features, others use characteristic clinical features, others use patients interpretations of their symptoms, and the rest use combinations of the above.

- Viner et al

Model incorporates snoring, BMI, age and gender. Used stepwise linear logistic regression.

- Maislin et al

Model incorporates snoring, gasping at night, witnessed apneas, age, gender and BMI. Multiple logistic regressions were used to generate a multivariable apnea risk register when compared to RDIs from polysomnographs. ROCs were used to test predictive ability.

- Metzger et al - Berlin Questionnaire

Model incorporates snoring, gasping at night, witnessed apneas, age, gender and BMI. Multiple logistic regressions were used to generate a multivariable apnea risk register when compared to RDIs from polysomnographs. ROCs were used to test predictive ability.

- Kirby et al Artificial Neural Nets

Uses 23 clinical variables including patients history, physical examination and patient reported sleepiness and smoking.

- Dixon et al

Looked at witnessed apneas, neck circumference and BMI. Study rather than a questionnaire.

- Kushida et al Kushida Index

Complicated morphometric model, including BMI, neck circumference, palatal height and oral cavity measurements amongst others. Suffers from being too complicated to be administered accurately and being time consuming.

- Tsai et al - upper airway physical examination protocol (UAPP)

Looked at six parameters, three clinical symptoms; snoring, witnessed apneas and hypertension and three measurable signs; cricomenal space, pharyngeal grade and overbite (info on these to follow)

- Chung et al STOP questionnaire

Four questions on snoring, daytime sleepiness, witnessed apneas and blood pressure.

- Chung et al STOPbang questionnaire

This is an extension of the STOP questionnaire that adds four additional questions on BMI, age, neck circumference and gender. A threshold of 3 out of 8 is generally used to indicate OSA.

- Meoli et al AASM OSA exploratory questionnaire

This questionnaire is referenced in a number of places however there is no data to back it up

- Chung et al ASA

Three categories are used to ask questions, physical characteristics, observed sleep disturbances and tiredness. It uses falling into two or more of these categories as an indicator of OSA.

- Flemons et al Flemons screening tool

This is a 36 question screening tool for OSA that uses a differential method for diagnosis, asking questions about depression and chronic diseases as well as the more common questions on tiredness, snoring and driving behaviour. Uses a weighted score called SACS with a threshold to indicate OSA.

- Johns Epworth Sleepiness Scale

A questionnaire using eight questions to assess sleepiness in different situations. Recommended by NHS guidelines.

5.3.4 Narrowing Down the Studies

A number of these are not formal questionnaires and therefore not known by the doctor negating one of the reasons for using a pre-existing questionnaire, however this isn't sufficient reason to rule them out. The Kushida Index and ASA questionnaire are complicated which goes against the design specification. A high negative predictive value is needed so the focus of more work will be on; Artificial Neural Net, UAPP and the STOPbang questionnaire. Epworth Sleepiness Scale will also be included in the app because it is part of the diagnostic pathway as laid out by the NHS.

5.4 Audio

5.4.1 Scoring of apnea R&K vs AASM

Audio signals taken during polysomnograms are currently scored by sleep specialists, there are two guidelines as to how to do this. The Rechtschaffen and Kales Manual is long standing, it was the only manual in use between 1968 when it was created and 2007 when the AASM Manual came into use. The R&K

manual is based on healthy subjects aged 21 to 86 years and doesn't actually mention how to recognise apneas. It has also been criticised for being open to interpretation. The AASM manual has a slight change in terminology and changes distribution of NREM sleep stages but the main difference is it explains how to classify more sleep abnormalities including apneas and arousals. The AASM scores a signal as an apnea if, there is a drop in the peak thermal sensor excursion by more than 90% of baseline, the event last at least 10 seconds and at least 90% of the events duration meets the amplitude reduction criteria for apnea. Obstructive apneas are associated with continued or increased inspiratory effort through the period of absent airflow. A minimum desaturation criterion is not required. The basis for scoring arousals is based on EEG and EMG and therefore isn't helpful in terms on how to analyse audio signals.

5.4.2 Methods of Analysis

There are a number of different methods that can be used to analyse audio signals, each will be looked at in turn, looking at how they work, studies on them and strengths and weaknesses of the method. Due to issues with background noise and other signal noise most methods focus on the characteristic snores of OSA sufferers rather than the quiet apneas.

Simple Characteristics

Three simple features of a snore can be analysed quite easily, snore duration, the time taken for a snore sound, generally measured in seconds; snore loudness, generally the average loudness measured from a microphone, a snore simulator is also needed in order to calibrate the microphone; snore periodicity, calculated from segmented short frames of the snores with low amplitude, high frequency components removed, autocorrelation used to assess each frame as either periodic or not. Overall periodicity calculated from the ratio of the number of periodic frames to the total number of frames.

Jones et al studies these features amongst others in order to see whether it was possible to predict the outcome of palatal surgery rather than as a diagnostic measure for OSA. Frame size of 200ms was used centre-clipped by 30%. Autocorrelation peaks between 25 and 87.5ms were used to classify as periodic.

Peak Power

Using Fast Fourier Transforms a power spectrum can be created of the snores. This can then be characterised in a number of ways including establishing: F_a the fundamental frequency; F_o the lowest frequency, F_{peak} the peak with the maximum power, F_{mean} the statistical mean frequency, and F_{max} can also be

calculated, however there are different conventions for this, it is defined as the frequency beyond which the signal amplitude has dissipated to less than a percentage of its peak power, some studies use 3% others 1%. Perez-Padilla et al used F_a , F_o , F_{peak} and F_{max} to examine the differences between nine OSA sufferers and ten simple snorers. Defining F_{max} as dissipating to 3% of peak power. Sound was recorded via a microphone attached to the manubrium sterni (chest). Significant variation was found between snores in a given patient making it hard to find a differentiator between OSA sufferers and simple snorers. It was found that for OSA suffers F_{peak} was usually at a higher frequency than F_a , however this was significant enough to be used to differentiate the two groups.

Fiz et al used F_{peak} , F_{mean} and F_{max} defined at 10% of peak power to distinguish between ten OSA sufferers and seven simple snorers. The microphone was placed just above the larynx without skin contact. Two features were found to distinguish OSA sufferers from simple snorers. The first was peak frequency (F_{peak}) which was significantly lower in OSA sufferers with a threshold of 150Hz, although one of each group was on the opposite side, a strong non linear negative correlation was seen between F_{peak} value and number of AHI events as seen in figure X (3), this is associated with a Spearman rank order correlation: $r=-0.70$; $p<0.0016$. The second feature was to do with the shape of the power spectrum. The simple snorers displayed a clear fundamental frequency and harmonic pattern whereas the OSA sufferers displayed a low frequency peak with scattered peaks over a narrow band of frequencies, Figure X (1 & 2 b) shows the different patterns. Fiz et al attributed the differences seen to microphone placement, Perez-Padilla et al placing their microphone on the chest whereas Fiz et al placing above the larynx, this results in a different filtering effect caused by the different tissues and cavities the sound travels through.

Power Ratio

Given the difference in spectra between those with OSA and simple snorers there is potential to characterise this by means of a cumulative power ratio. This would be the area under one part of the power spectrum divided by the area under the rest, where the threshold(s) is placed would depend on what characteristic was trying to be differentiated. From the power spectrum from the Fiz et al study above one potential threshold would be 100Hz to pick up on the low frequency components of the OSA curve, see figure X (adapted version of 1&2 b from Fiz). Perez-Padilla et al used superimposed spectra from ten snores from each subject (9 OSA, 10 simple snorers) and a threshold of 800Hz, dividing the integral of the spectra above 800Hz with that below 800Hz, for OSA patients who took a second breath after an apnea the cumulative power ratio was also calculated for that. Figure X (8) shows the scattering of the ratios,

with snorers having a ratio of 0.08 ± 0.02 and OSA sufferers a ratio of 1.12 ± 0.31 . A threshold of 0.3 was proposed which would distinguish all but one OSA sufferer on first breath after apnea, this patient had a low AHI and mild symptoms. Hara et al used the same method as above on 46 OSA sufferers and 12 simple snorers, keeping the threshold at 800Hz, using a ratio of below 800Hz to above 800Hz. Simple snorers had a power ratio of 34.002 whereas OSA sufferers had a ratio of 6.288. The p value of a Mann-Whitney U test was 0.015, this small value is a good indicator that this didn't happen by chance. Hara et al wouldn't recommend this approach as the calculation is very time consuming. Significant differences were found between the values of the ratios in both studies although in both cases a difference between OSA sufferers and simple snorers was clearly seen.

Sound Intensity

Another diagnostic tool uses sound intensity without frequency, instead looking at the apnea-snoring combination. Define an acoustic signature event (ASE) as a period of apnea, duration specified between limits, followed by snoring, where snoring and apnea are defined in terms of sound intensity. Van Brunt DL et al define apnea below 50microV and snoring above 100microV with apnea episode lasting between 10 and 90 seconds. 30 second intervals were analysed by sound intensity and polysomnogram and analysed in two ways. Firstly each patient (69 patients, 51 OSA suffers, 18 not) was assessed independently and RDI score compared with predictions, for an RDI of 15/hour or greater sensitivity was 0.93, specificity 0.25, false positive 36.2%, false negative 2.8%, 60.9% classified correctly. Secondly pooling all the observations (60231) resulting in a 33% sensitivity, 98% specificity, 85% classified correctly.

Formants

Formants are the resonant frequencies of the signal, most easily determined by picking out the peaks on a linear predictive coding (LPC) spectrum of the signal. LPC is the spectral envelope produced by a linear predictive model. The lowest formants are associated with degree of constriction of the pharynx, degree of advancement of the tongue and degree of lip rounding respectively, these are often referred to as F1, F2 and F3. Because these physical properties change in sufferers of OSA there is a chance that the frequencies associated with them will change too, therefore threshold frequencies to distinguish OSA sufferers and simple snorers are sought.

Ng et al tested 30 OSA sufferers and ten simple snorers and found a threshold for F1 of 470Hz but not F2 nor F3, this threshold yielded a sensitivity of 88% and a specificity of 82%. However increased

sensitivity and specificity were seen if different thresholds were used for men and women as seen in table X (1). Women show a greater distinction in F1 frequency than men as well as a reduced spread of results, although more outliers amongst the simple snorers, as seen in figure X (1). It is however worth noting that the sample size for women was small (6 OSA sufferers, 4 simple snorers) Once the threshold has been established an equation is needed to convert it to an AHI value, a number of equations were proposed and regression used to see which was the best fit, as seen in table X(2). A power law came out best with a regression of 0.5334 giving a predicted AHI score of 12.2 when 10 was being aimed for. It is worth noting that the same subjects was used for training and testing, although different data for each.

Sola-Soler et al used formant frequencies to distinguish between snores from eight simple snorers (447 snores) and eight OSA sufferers (236 normal snores and 429 post-apneic snores). The spectral envelope was estimated by linear predictive autoregression, with very low amplitude spurious peaks rejected by a 3dB threshold. Investigation of the spectral envelope found 2 to 6 formants in each snore, these fell in common frequency range around 150Hz, 500Hz, 1KHz, 1.7KHz, and in a few snores 2.2KHz. This led to definition of five frequency bands: B1[0,300), B2[300,700), B3[700,1400), B4[1400,1900) and B5[1900,2500) in Hz. For each band and type of snore (simple snorer SN, OSA normal snore OP-N, and OSA post apneic snore OP-PA) the mean value F_i and standard deviation SF_i was calculated. Table X (3) shows a comparison between these means and standard deviations for each combination of snore type calculated using the Mann-Whitney U test, the fifth band was left off because so few snores exhibited this formant. If a snore had more than one formant in a band the average frequency of those was used in the calculation. Bands 1 & 3 showed significant differences between formants when comparing the standard deviation of simple snorers and OSA sufferers both in normal snores and post apneic snores of the OSA sufferers. The most distinct difference was between the standard deviation of simple snorers normal snores and post-apneic snores in band 1 which had a probability of 0.0006.

Yadollahi et al used formant frequencies to distinguish between snores and breaths rather than simple snorers and OSA suffers so a direct comparison of method cannot be made however there is value in exploring the method used. Bands were used as in the Sola-Soler study but at different frequency ranges, [20400]Hz, [270840]Hz, [5001380]Hz, [9101920]Hz, [1680-2680]Hz, [2580-3770]Hz and [3590-5000]Hz these were found using Kmeans clustering. This is a method of partitioning data unsupervised, it uses an iterative method to find a predefined number of partitions, in this case seven, an error margin of 10^5 was used for the iterations. The process is sensitive to initial conditions so was repeated 20 times with different initial conditions, the one with the minimum error was selected. Table X (3) shows the student

t-test p values, which show the first and third formants to be significant, with probability $p = 0.003$ and $p = 0.0244$ respectively. The F1 frequency of the breath sound was greater than that of the snore while the F3 frequencies with the converse.

Bispectral Analysis

Bispectral analysis exploits the fact that the bispectrum reveals both amplitude and phase information about a spectrum, while also being calculated by convolution makes it the easiest polyspectra to compute. Polyspectra are Fourier Transforms of cumulants, for example the second order cumulant; autocorrelation Fourier Transforms to the Power Spectrum. The third-order cumulant $C(m,n) = E x(k)x(k+m)x(k+n)$ transforms via a Double Discrete Fourier Transform (DDFT) to the bispectrum. Although the bispectrum is often plotted on a square it is symmetric and so only a triangular region is needed to completely describe it, this is defined by $0 \leq \omega_2 \leq \omega_1, \omega_1 + \omega_2 \leq \pi$

Quadratic phase coupling occurs uniquely in second-order non-linear systems, and is where the phases add and subtract along with the frequency components. (QPC) causes peaks in the bispectrum triangular region, this shows energy is produced at frequency $\omega_1 + \omega_2$, a flat bispectrum at ω_1 and ω_2 suggests no activity and that it is not affected by QPC.

Ng et al exploited the bispectrum shape in order to distinguish between nine OSA sufferers and seven simple snorers. Bispectral analysis has benefits over power spectrum because it reveals the non-Gaussian and non-linear behaviour, given the upper airway is non-linear this is a good plan.

Noise was suppressed using a level-wavelet-dependent (LWD) thresholding scheme under undecimated discrete wavelet transform (UDWT) setting. Fast Fourier Transforms were used to estimate the bispectrum, this was plotted (figures X and X (4 & 5) and inspected visually, the axes have been normalized with a frequency of 1 being 11025Hz. From visual inspection it appears the biggest peak for simple snorers are near the origin while for apneic snores are further away, this suggests a greater degree of phase coupling in apneic snores due to nonlinearities in the signals. When analysed peak position was reflected in the numbers with apneic peaks are higher frequencies than simple snore peaks, table X(1) shows the figures.

Clustered multiple comparison graphs were then produced, figure X(6), QPCs appear mainly at $f_1 = f_2$ for simple snores whereas they appear mainly at $f_1 \neq f_2$ for apneic snores, however there is less self coupling. 77% of simple snore are self coupled compared to 49% of apneic snores. So the analysis shows there are three differences between simple snores and apneic snores, apneic snores have strong presence

of nonlinear interaction, less self-coupling and QPC peaks appear and higher frequencies.

Wavelet Analysis

Translation-Invariant Discrete Wavelet Transform(TIDWT) is a nonorthogonal, undecimated adaption of the more common Discrete Wavelet Transform (DWT) which is orthogonal and maximally decimated, and causes Gibbs like artefacts around discontinuities. There are two TIDWT methods: ‘a-trous and cycle-spinning. The ‘a-trous scheme removes the downsamplers and upsamplers of the DWT and upsamples the filter coefficients by a factor of s^{j-1} in the j^{th} level of the algorithm. As the output of each level contains the same number of samples as the input it is inherently redundant.

Cycle spinning incorporates translation invariance by applying DWT to all circular shifts of the input vector and averaging over them. However due to periodic properties the number of shifts reduces to one. Both schemes offer better error properties than DWT due to redundant coefficients by about 10-20

Ng et al used cycle spinning TIDWT to distinguish between 30 OSA sufferers and ten simple snorers. Ten snores of about 6 seconds were randomly chosen from each snorer, marked by polysomnogram technologists. Figure X(5) compares the energy approach used by Cavusoglu et al and the TIDWT approach used by Ng et al in this study. At the narrowest tolerance of 25ms the TIDWT approach detected 51% of the snore segments correctly compared with 8% for the energy approach, and at the largest tolerance of 125ms the TIDWT approach detected 98% correctly, whereas the energy approach only managed 87%, i.e. the TIDWT approach is at least 10% more effective.

Multiscale Entropy Coefficients

Entropy is used as a measure of complexness and the idea of using entropy for multiple scales was originally proposed by Zhang however this was based on Shannons definition of entropy that has some flaws so Costa et al proposed a new method using sample entropy (SampEn) a refinement on approximate entropy (ApEn) introduced by Pincus .

The method works by constructing consecutive coarse-grained time series of the original time series. These are created by averaging the data points within non-overlapping windows of increasing length. Each element of the coarse-grained series is calculated by the equation . An illustration of this is shown in figure X (1)

SampEn is then calculated for each coarse-grained time series and plotted as a function of the scale factor. SampEn quantifies the regularity and predictability of the time series, it acts as a regularity

statistic, looking for patterns, it does this by looking at the probability that m consecutive data points that are similar will remain similar when one more data point is added, here similar means the distance between them is less than r .

Roebuck and Clifford used MSE over 40 scales (1-40seconds) to distinguish between 50 simple snorer, 72 OSA sufferers and 24 normal subjects. They used 240minutes of recording from each subject, splitting the data between a training set and a testing set 70:30. Scales of 6seconds, 21seconds and 30second yielded a specificity of 92.5% and a positive predictive value of 85.8% in the training set and a specificity of 90.5% and a positive predictive value of 83.5% in the testing set.

5.5 Signal Analysis – simple method

5.5.1 Outline

The simple method of diagnosing sleep apnea, using audio data from the user’s phone that is recorded while he/she is sleeping, was meant to provide a starting point for the development of the app. It served three main purposes:

- To familiarise us with the typical sleep patterns and with power and frequency content of sleep data
- As a backup

This would give us a method that is able to provide a diagnostic output such as the apnea-hypopnea index score from sleep data, even if it was not using machine learning algorithms.

- As a point of comparison

The simple method would serve as a point of comparison, along with other methods used, with regards to the accuracy of the diagnosis. Using simple metrics such as percentage accuracy of pre-determined apnea or hypopnea points in the data against what the model is able to pick out, we can compare the simple model results with our machine learning results. This would allow us to gauge our performance and also prove that the app is able to diagnose OSA with superior accuracy.

MATLAB[®] was used as the development environment for the simple model. This was due to several reasons. Firstly, our familiarity with MATLAB[®] from previous projects made it a natural starting point. Secondly, as a dynamically typed language with a user-friendly interface, MATLAB[®] would enable us to make minor changes to the code and observe the results quicker. Experimentation and tinkering with the code is much easier in MATLAB[®] than it is in C/C++ or Java, for example. This ease of experimentation meant that MATLAB[®] is a good language to start writing the model in, and is used in the initial development of the machine learning HMM model as well. With in-built functions such as `audioread`, MATLAB[®] provided the basic tools with which we could develop the model. Of course, if necessary, the model could later be written in Java for implementation in an Android App - this would be trivial.

The MATLAB[®] code for the simple model is presented below, with detailed explanations. A brief summary is as follows: three .m files are created - `simple.m`, the main script which is run once an audio file is created and stored, and two functions `detectApnea.m` and `detectApneaVar`, that take a vector of the signal power and a few other parameters as inputs. The `simple.m` script uses the `wavread` or

audioread function (the user's audio sleep data is recorded in .wav format) to read the file and produce a matrix of the audio level values. This is sampled at a lower frequency in order to reduce memory storage. The frequency content of the signal is calculated using the fast fourier transform function (FFT) Along with a plot of the signal, a plot of the frequency content is generated (this is done purely for the programmer's convenience and analysis). The power content is calculated from the signal vector and is used in the detectApnea function. An additional function, detectApneaVar, is included in the code below highlighting two different ways of analysing the data. The first way, used in detectApnea, uses a simple threshold parameter, and searches the signal power vector for prolonged periods of time when the value is below a threshold level. These periods represent apneatic episodes when the user's airflow experiences blockages. The second way, used in detectApneaVar, aims to identify the sudden inspiration that accompanies the body attempting to re-establish airflow. This is usually characterised by a snorting noise from the user. Instead of simply looking at the power values and comparing them to a threshold, detectApneaVar identifies periods of high variance in the signal, which represent the user being 'shocked' to start breathing again.

5.5.2 Implementation in MATLAB®

```
1 % Reading data
2 clear all;
3 close all;
4 FILENAME = 'signal.wav';
5 [YRaw,f] = audioread(FILENAME) ;
6 TMAX = length(YRaw) / f;
7
8 % Sampling data because we don't need very high resolution
9 scale = 20;
10 for i = 1:(length(YRaw) / scale)
11     Y(i) = 0.5 * (YRaw(i * scale, 1) + YRaw(i * scale, 2));
12 end
13
14 % Plots sampled data
15 figure;
16 plot(Y);
17 title('Sleep signal');
```

```

18
19 % Calculates and plots frequency
20 N = length(Y);
21 Yf = fft(Y,N);
22 freq = ((0:1/N:1-1/N)*f).'; % Frequency vector;
23
24 % Plot spectrum.
25 plot(freq,abs(Yf))
26 title('Amplitude Spectrum of y(t)')
27 xlabel('Frequency (Hz)')
28 ylabel('|Y(f)|')
29
30 % Calculates and plots the power
31 power = Y.^2;

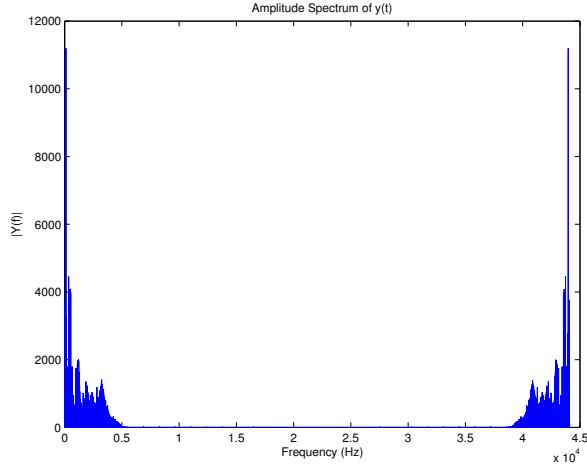
```

The first part of the code above assumes that the user's sleep data has already been recorded using the microphone and has been stored in a file `signal.wav`. This file is read using the `wavread` function as mentioned, and outputs `YRaw`, a two-column matrix (as wav encoding uses two channels) as well as `f`, the sampling frequency which is 44.1 kHz. The length of the audio file in seconds, `TMAX`, is also calculated for later use.

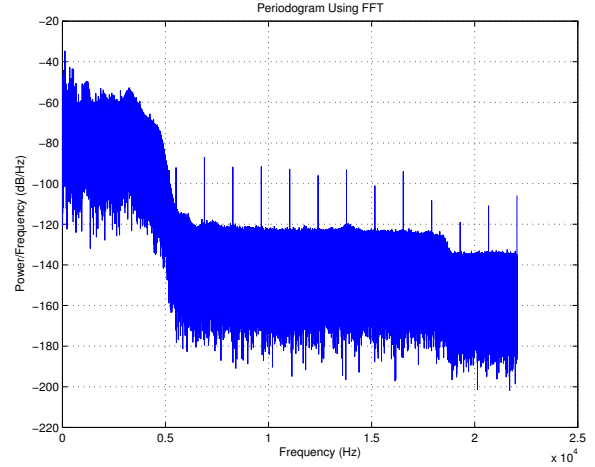
A sampling frequency of 44.1 kHz is unnecessarily large and wasteful for an application such as ours - the frequency content of a 7-minute sample obtained from YouTube [5] is shown below. The figure on the left represents the spectral density while that on the right represents the information on a logarithmic scale so as to highlight where the useful information is found. As can be seen, there is no useful information that can be found at frequencies above 5 kHz (the duplicated spectra on the left are a result of sampling at the frequency of 44.1kHz). There is no risk of aliasing occurring even if the audio is sampled at 5 kHz. This is where the scale parameter in line 9 above comes in - it reduces the size of `YRaw` by sampling the already sampled vector (and also combines the two channels into one by taking the average).

The frequency content shown above is calculated using the fast fourier transform (FFT) function in MATLAB[®]. The function calculates the discrete fourier transform (DFT) of a vector $\mathbf{x} = \{x_1, x_2, \dots, x_N\}$ and returns output $\mathbf{X} = \{X_1, X_2, \dots, X_N\}$ such that

$$X(k) = \sum_{j=1}^{j=N} x(j) \omega_N^{(j-1)(k-1)} \quad (5.1)$$



(a) Amplitude Spectra of Raw Audio File



(b) Periodogram of Raw Audio File

Figure 5.1: Frequency content of Raw Audio File

where

$$\omega_N = e^{(-2\pi i)/N} \quad (5.2)$$

The next few lines of code above serve to calculate and plot, again, the frequency of the reduced vector Y (the figures above are for Y_{Raw}). The vector power is also created to hold values for the power of the signal at each time period, and will be used in the functions `detectApnea` and `detectApneaVar`.

The next part of the script sets some parameters and uses `detectApnea` as well as `detectApneaVar` to analyse the signal power. The results are then put together and plotted for the programmer's benefit. (The code for doing so is not shown here as it is relatively straightforward and unimportant)

```

1 % Apnea detection
2 sensitivityMean = 0.01;
3 interval = 3;
4 sensitivityVar = 5e-2;
5 windowSize = 20;
6 apnea = detectApnea(power, TMAX, sensitivityMean, interval);
7 apneaVar = detectApneaVar(power , TMAX , sensitivityVar , windowSize);

```

The function `detectApnea` takes as inputs the vector power, the length of the audio file `TMAX`, and parameters `sensitivityMean` and `interval`. The code for `detectApnea` is shown below:

```

1 function apnea = detectApnea(Y, TMAX, sensitivityMean, interval)
2
3     n = length(Y);    % No. of samples
4     sampleInterval = round(n / TMAX * interval);
5     % Minimum no. of consecutive samples that should be below threshold for apnea
6     apnea = zeros(1, n);
7     % Generate a vector that will contain either zeros or ones to show where apnea is
8
9     threshold = mean(Y) / sensitivityMean;
10
11     nBelowThreshold = 0;    % Number of sample points below the threshold in a row.
12     for i = 1:n
13         if Y(i) ≤ threshold
14             nBelowThreshold = nBelowThreshold + 1;
15     % Increase # of sample points below the threshold in a row
16         else    % We see a point that is above threshold.
17             if nBelowThreshold ≥ sampleInterval    % Condition for which we classify ...
18                 apnea.
19                 for j = max((i - nBelowThreshold), 1):(i - 1)
20     % Loop through the last 'nBelowThreshold' points. Making sure (i - nBelowThreshold) ...
21                 doesn't go below 1 (otherwise error).
22                 apnea(j) = 1;
23             end
24         else
25             for j = max((i - nBelowThreshold), 1):(i - 1)
26                 apnea(j) = 0;
27             end
28         end
29     end
30 end

```

Taking inputs `sensitivityMean` and `interval`, `detectApnea` runs through the vector `power` and identifies when the signal power is below a threshold level for at least a certain interval. This threshold level can be adjusted by changing `sensitivityMean`, and also is affected by the mean value of the overall signal power. This is important, as it is a first step towards ensuring that variations due to users putting the phone

further away, which would reduce the overall power of the signal, are taken care of to some extent. The output vector `apnea` contains ones and zeroes at every sample point, with ones representing apnea or hypopnea episodes.

Instead of simply searching the vector power for values lower than a threshold, `detectApneaVar` attempts to identify periods when there is a sudden spike in the signal power, which means the user has snorted and been shocked into breathing again. Similar to `detectApnea`, `detectApneaVar` uses parameters such as `sensitivityVar` and `windowSize`. The code for `detectApneaVar` is presented below:

```
1 function apnea = detectApneaVar (Y , TMAX , sensitivityVar , windowSize)
2
3 n = length (Y);
4 apnea = zeros (1 , n);
5
6 % Calculate variance of whole signal (as a yardstick)
7 variance = var(Y) ;
8 maxVariance = variance / sensitivityVar;
9
10 % Calculate the variance through a moving window
11 twindow = [1:windowSize ; Y( 1:windowSize )];
12 % This vector contains the locations of the moving window
13
14 for i = 1:( n-windowSize )
15
16     sigma2 = var( twindow(2, :) );
17
18     if sigma2 > maxVariance
19         apnea(1 , twindow(1,:) ) = 1;
20     end
21
22     twindow(1,:) = twindow(1,:) + 1; % Update the window for the next round of ...
        variance calculations
23     twindow(2,:) = Y ( twindow(1,:) );
24
25 end
```

As can be seen, a variance method is used to detect sudden spikes in the signal. A moving window is created of size `windowSize` and is used to temporarily house parts of the vector `power`. The variance of the values in the window is calculated and if it exceeds a value `maxVariance`, the user is recognised as having had an apnoeatic episode. The window moves on to the immediate next period after updating the output vector `apnoea`, and by the end the vector `apnea` contains ones and zeros identifying points in the signal where apnoea is thought to have occurred. Once again, variations due to different users and settings have been accounted for to a certain extent by calculating the value of `maxVariance` from the variance of the entire signal.

The results from the two methods of detecting apnoea are combined together, and the results are plotted below for the sample YouTube video. Firstly, the plot of the power signal, with peaks at regular intervals, confirms that the user has OSA and experiences apnoea and hypopnoea in predictable cycles. The results from the two methods are plotted below the power signal, and exhibit enough correlation such that combining the methods can be justified.

5.5.3 Limitations of model

While the simple model we have used above gave us a good starting point and will serve as a point of comparison, it has many limitations. Firstly, the choice of parameter values plays a huge role in the accuracy of the diagnosis. Even though some effort at reducing the effect of variations in noise and signal strength has been taken, the choice of `sensitivityMean`, `sensitivityVar`, `interval` and `windowSize` is still arbitrary to a large extent. This means that while the model works well for the sample above, there is no guarantee of its effectiveness for other audio signals.

This is where machine learning comes in - needing to choose arbitrary parameter values is removed as the program can be designed to learn, with training data, the best values for parameters and update itself accordingly. The parameters do not have to be the same as those above, of course - this would depend on the exact machine learning model being used.

Secondly, the simple model assumes the existence of an audio file that has already been recorded. Given the average sleep time for adults of seven hours, this could lead to memory storage issues in smartphones where the recording is meant to take place. Some form of compression of the data needs to take place even while recording, and this issue is tackled in the following sections of the report.

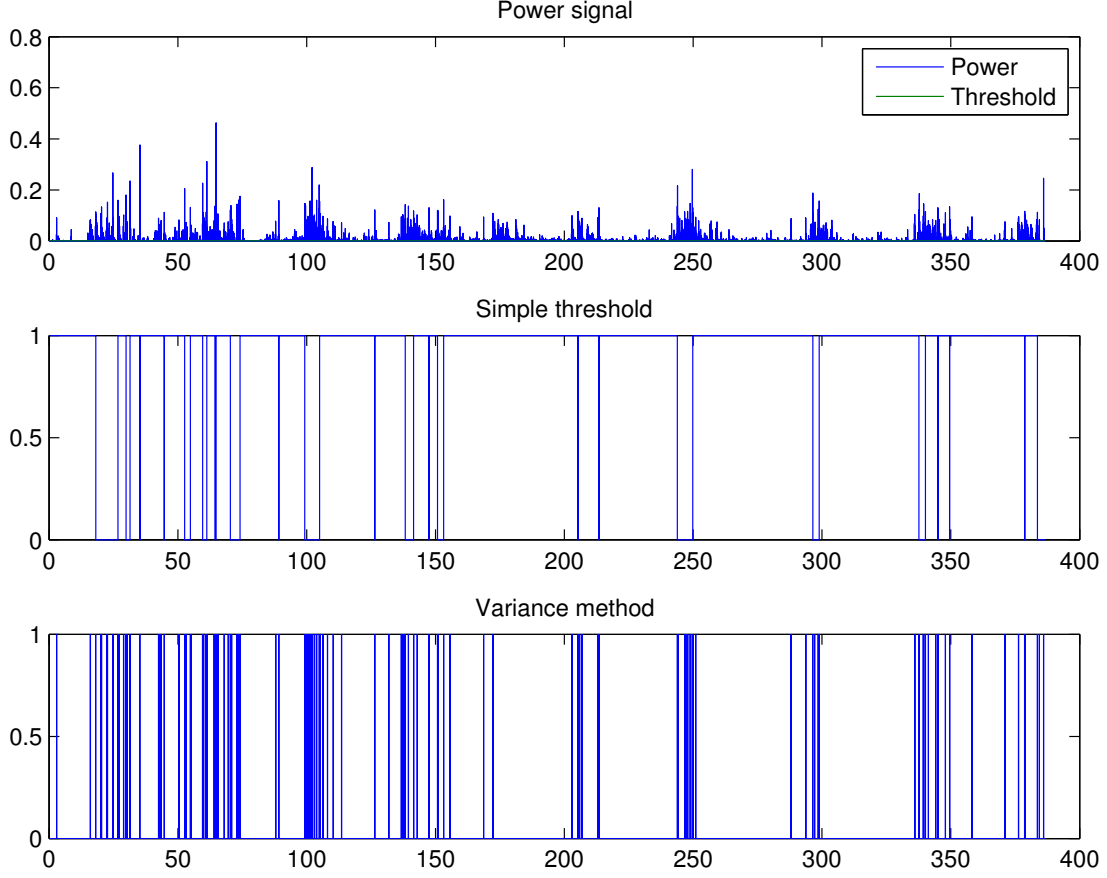


Figure 5.2: Diagnosis Results from 7-minute Sample

5.6 Machine Learning – Theory

Machine learning, a branch of artificial intelligence, concerns the construction and study of systems that can learn from data [21]. The supervised classification problem in machine learning concerns finding the unknown target function that classifies certain input data into classes based on some set of training examples containing labelled input data.

It is exciting to use machine learning algorithms to aid medical diagnoses because it can dramatically save time for medical experts. These techniques should create a reasonably reliable, though not perfect, system on which the medical experts can base their decisions on.

In our case, given a sampled sound signal of a sleeper, we want to identify apnoea periods. In particular, we represent our input (sampled sound signal) as $\mathbf{S} = \{s_1, s_2, \dots, s_T\} \equiv \{s_i\}_{i=1}^T$, and we want to output the classifiers for every K samples, $\mathbf{Y} = \{y_i\}_{i=1}^{T/K}$, where the classifier $y_i \in \{0, 1\}$ corresponds

to samples $\{s_j\}_{j=(i-1)K+1}^{iK}$ of the signal. We assume that T is divisible by K , however if this is not the case, we discard an appropriate number of signal samples to fulfill this condition.

We have researched three models for our problem which we will discuss in this section. Firstly, we will discuss Support Vector Machines which are one of the most widely used algorithms in Machine Learning today, then we will discuss the State-Space Model and the Hidden Markov Models, which are more well-suited to our problem due to their temporal nature. Moreover, we discuss techniques to condition our data before using them as input data for our learning models.

5.6.1 Support Vector Machines

Here, we present the theory for Support Vector Machines (SVMs) based on the lecture notes from Prof. Andrew Ng [8]. SVMs are one of the most widely used and many argue among the best “off-the-shelf” supervised learning algorithms. This is mainly due to the sound theoretical framework, efficiency and good generalisation guarantees even for high-dimensional and linearly non-separable data.

Notation

Having m training examples, where

- $\mathbf{x}^{(i)} \in \mathbb{R}^d$ is the d -dimensional i -th training example.
- $y^{(i)} \in \{-1, 1\}$ is the i -th training label.

we want to find the parameter $\mathbf{w} \in \mathbb{R}^d$ which describes the hyperplane $\mathbf{w}^T \mathbf{x} + b = 0$ that separates our two classes. Thus, we can define our classifier as $h_{\mathbf{w},b}(\mathbf{x}) = g(\mathbf{w}^T \mathbf{x} + b)$, such that $g(z) = 1$ if $z \geq 0$ and $g(z) = -1$ otherwise. Note that this is a non-probabilistic learning model as we are not considering the probability of each class or the data.

Objectives

The essence of SVMs lies in finding the decision boundary (hyperplane) which maximises the gap between the closest training points to it. For the i -th training point $x^{(i)}$, we call the “gap”, geometric margin $\gamma^{(i)}$, which is the distance to the decision hyperplane and can be found by considering a point \mathbf{x} on it (note

that $\mathbf{w}^T \mathbf{x} = -b$):

$$\begin{aligned}\gamma^{(i)} &= \left| \frac{\mathbf{w}^T}{\|\mathbf{w}\|} (\mathbf{x}^{(i)} - \mathbf{x}) \right| \\ &= \frac{1}{\|\mathbf{w}\|} y^{(i)} (\mathbf{w}^T \mathbf{x}^{(i)} + b)\end{aligned}$$

However, we only consider the closest point $\mathbf{x}^{(i^*)} : i^* = \arg \min_i \gamma^{(i)}$ with the geometric margin of $\gamma = \min_i \gamma^{(i)}$. Since scaling \mathbf{w} and b does not change the output of the classifier, nor the geometric margin $\gamma^{(i)}$, for convenience, we decide to scale \mathbf{w} and b such that $|\mathbf{w}^T \mathbf{x}^{(i^*)} + b| = y^{(i^*)} (\mathbf{w}^T \mathbf{x}^{(i^*)} + b) = 1$. Thus, maximising the geometric margin of the closest point becomes

$$\begin{aligned}\max_{\mathbf{w}, b} \quad & \frac{1}{\|\mathbf{w}\|} \\ \text{s.t.} \quad & y^{(i)} (\mathbf{w}^T \mathbf{x}^{(i)} + b) \geq 1, \quad i = 1, \dots, m.\end{aligned}$$

which is equivalent to

$$\begin{aligned}\min_{\mathbf{w}, b} \quad & \frac{1}{2} \|\mathbf{w}\|^2 \\ \text{s.t.} \quad & y^{(i)} (\mathbf{w}^T \mathbf{x}^{(i)} + b) \geq 1, \quad i = 1, \dots, m.\end{aligned} \tag{5.3}$$

The solution to the optimisation problem (5.3), which can be found using off-the-shelf Quadratic Programming (QP) packages, gives us the parameters required to do classification.

Lagrange duality

While solving the optimisation problem (5.3) using QP solves the problem, we move on to derive the dual form of the problem using the principle of Lagrange duality, which will help us to solve the problem using a more efficient algorithm. More importantly, it will also allow us to efficiently transform the data points to high-dimensional spaces using the “kernel trick”, capturing the non-linear nature of the decision boundary without losing the generalisation guarantees. The Lagrangian of our primal minimisation problem (5.3) (with parameters $\boldsymbol{\alpha} \in \mathbb{R}^m$) can be formed as

$$\mathcal{L}(\mathbf{w}, b, \boldsymbol{\alpha}) = \frac{1}{2} \|\mathbf{w}\|^2 - \sum_{i=1}^m \alpha_i \left[y^{(i)} (\mathbf{w}^T \mathbf{x}^{(i)} + b) - 1 \right] \tag{5.4}$$

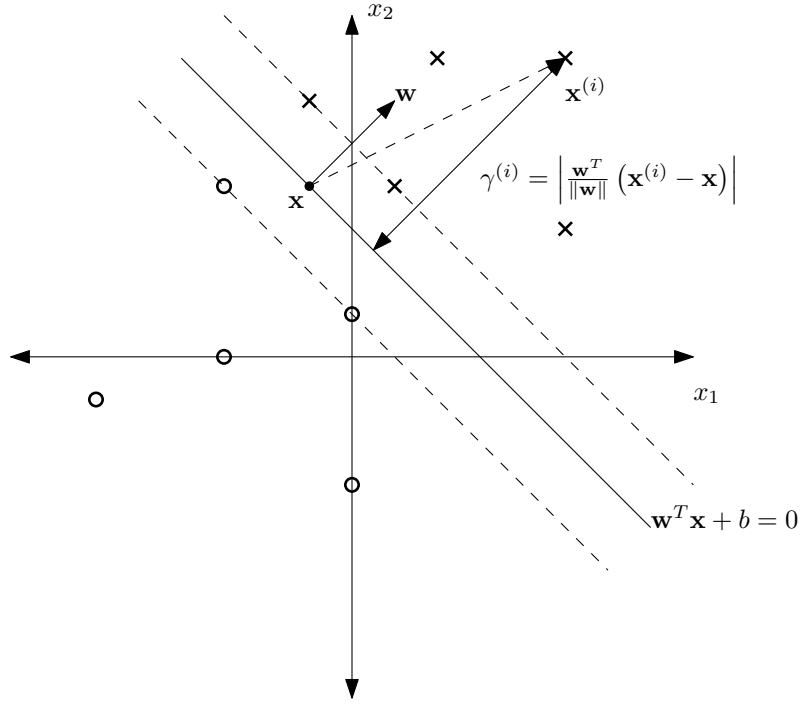


Figure 5.3: Illustration of the optimal margin classifier.

To find the dual form of the problem, $W(\alpha) = \min_{\mathbf{w}, b} \mathcal{L}(\mathbf{w}, b, \alpha)$, we find the gradients of (5.4) with respect to \mathbf{w} and b and set them to zero to get

$$\mathbf{w} = \sum_{i=1}^m \alpha_i y^{(i)} \mathbf{x}^{(i)} \quad (5.5)$$

$$\sum_{i=1}^m \alpha_i y^{(i)} = 0 \quad (5.6)$$

Substituting (5.5) and (5.6) back to (5.4) gives us the dual form, $W(\alpha)$

$$W(\alpha) = \sum_{i=1}^m \alpha_i - \frac{1}{2} \sum_{i,j=1}^m y^{(i)} y^{(j)} \alpha_i \alpha_j \langle \mathbf{x}^{(i)}, \mathbf{x}^{(j)} \rangle \quad (5.7)$$

Thus, under certain conditions which are in this case fulfilled (and omitted for clarity), our original optimisation problem (5.3) becomes equivalent to the dual optimisation problem

$$\begin{aligned} \max_{\alpha} \quad & W(\alpha) \\ \text{s.t.} \quad & \alpha_i \geq 0, \quad i = 1, \dots, m \\ & \sum_{i=1}^m \alpha_i y^{(i)} = 0, \quad i = 1, \dots, m \end{aligned} \quad (5.8)$$

This problem can be solved using a QP algorithm, however a more efficient Sequential Minimal Optimization (SMO) algorithm can be used. Once the optimal value α^* is obtained, we can find the corresponding parameters of the SVM \mathbf{w}^* using (5.5) and b^* using

$$\begin{aligned} b^* &= -\frac{\max_{i:y^{(i)}=-1} \mathbf{w}^{*T} \mathbf{x}^{(i)} + \min_{i:y^{(i)}=1} \mathbf{w}^{*T} \mathbf{x}^{(i)}}{2} \\ &= -\frac{\max_{i:y^{(i)}=-1} \sum_{j=1}^m \alpha_i^* y^{(i)} \langle \mathbf{x}^{(i)}, \mathbf{x}^{(j)} \rangle + \min_{i:y^{(i)}=1} \sum_{j=1}^m \alpha_i^* y^{(i)} \langle \mathbf{x}^{(i)}, \mathbf{x}^{(j)} \rangle}{2} \end{aligned} \quad (5.9)$$

Thus the classification of a test point \mathbf{x} can be done by evaluating the argument of $g(\mathbf{w}^{*T} \mathbf{x} + b^*)$

$$\mathbf{w}^{*T} \mathbf{x} + b^* = \sum_{i=1}^m \alpha_i^* y^{(i)} \langle \mathbf{x}^{(i)}, \mathbf{x} \rangle + b^* \quad (5.10)$$

We note that due to certain conditions (Karush-Kuhn-Tucker conditions) the α_i^* 's that are non-zero correspond to the $\mathbf{x}^{(i)}$'s that lie on the margin. We call these points the Support Vectors (SVs).

Kernel trick

Note that according to (5.10) (and (5.9)), we only need to evaluate the inner products of \mathbf{x} and the support vectors in order to classify the point \mathbf{x} . This fact is used in the “kernel trick”, in which a kernel function $K(\mathbf{x}, \mathbf{z})$ is used as a proxy for the inner product $\langle \mathbf{x}, \mathbf{z} \rangle$. This effectively simulates transforming the data points to another, possibly unknown, space via a transformation function $\phi(\cdot) : \mathbb{R}^d \rightarrow \mathcal{Z}$ as long as there exists such \mathcal{Z} , i.e. there exists $\phi(\cdot)$ such that $K(\mathbf{x}, \mathbf{z}) = \phi(\mathbf{x})^T \phi(\mathbf{z})$. It can be shown that a kernel $K(\cdot, \cdot)$ is valid if and only if it satisfies certain conditions called the Mercer's conditions. This allows us to transform our input domain into much higher dimensional domains without actually doing so which turns out to improve the time complexity significantly.

$$K_{\text{poly}}(\mathbf{x}, \mathbf{z}) = (a\mathbf{x}^T \mathbf{z} + c)^k \quad (5.11)$$

$$K_{\text{rbf}}(\mathbf{x}, \mathbf{z}) = \exp\left(-\frac{\|\mathbf{x} - \mathbf{z}\|^2}{2\sigma^2}\right) \quad (5.12)$$

In our application, we are going to use the kernels above (5.11, 5.12). The first one, (5.11), is the polynomial kernel which effectively transforms the input domain space into a feature space whose features are products all possible permutations of the input features of degrees up to k . The second one, (5.12), is a radial basis kernel (RBF), whose corresponding transformation function transforms the input domain

space to an infinite dimensional one. This kernel gives a large inner product to two points if they are close to each other.

Soft margin SVMs

Soft margin SVMs are a slight modification of the original problem that allows small violations of the margin. The purpose is to guarantee that the algorithm doesn't fail because of the non-separability of the input data even after using the kernel trick. In practice, these two techniques are used simultaneously. It turns out that only minor changes arise and the SMO algorithm can still be used.

Our problem

In our problem, we are going to use the **SVM** package in **MATLAB**[®] in order to train our model and classify sleep apnoea. The package includes implementations of both **QP** and **SMO** algorithms, as well as various kernels, including the polynomial kernel and the RBF kernel. Recall that in our problem, we have the signal $\{s_i\}_{i=1}^T$ and the classifiers for every K samples $\{y_i\}_{i=1}^{T/K}$, where $y_i \in \{0, 1\}$ classifies the time period represented by $\{s_j\}_{j=(i-1)K+1}^{iK}$. When using SVMs, the input vectors and the classifiers become

$$\mathbf{x}^{(i)} = [s_{(i-1)K+1}, \dots, s_{iK}]^T$$

$$y^{(i)} = \begin{cases} 1 & \text{if } y_i = 1 \\ -1 & \text{otherwise.} \end{cases}$$

5.6.2 State-Space Models

Here, we present the State-Space Models (SSMs) (also known as Linear Dynamical Systems) based on Kevin Murphy's book [7, Chapter 18] and Prof. Zoubin Ghahramani's paper [2]. SSMs allow us to model systems that are dynamic. Unlike the SVMs, SSMs will model dependencies of the current state on the previous ones.

We have two set of random variables, the hidden states $\mathbf{X} = \{\mathbf{x}_t, \mathbf{x}_t \in \mathbb{R}^d\}_{t=1}^T$ and the observed vectors $\mathbf{Y} = \{\mathbf{y}_t, \mathbf{y}_t \in \mathbb{R}^k\}_{t=1}^T$. We can represent SSMs graphically in a Bayesian network in Figure 5.4, and write out the joint probability of the model as

$$p(\mathbf{X}, \mathbf{Y}) = p(\mathbf{x}_1)p(\mathbf{y}_1|\mathbf{x}_1) \prod_{t=2}^T p(\mathbf{x}_t|\mathbf{x}_{t-1})p(\mathbf{y}_t|\mathbf{x}_t) \quad (5.13)$$

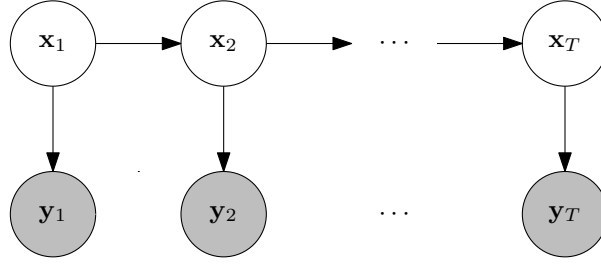


Figure 5.4: Probabilistic Graphical Model of a SSM and a HMM

In our case, we consider these particular transition and observation models with zero-mean Gaussian noises:

$$\mathbf{x}_t = \mathbf{A}\mathbf{x}_{t-1} + \mathbf{w}_t \quad (5.14)$$

$$\mathbf{y}_t = \mathbf{C}\mathbf{x}_t + \mathbf{v}_t \quad (5.15)$$

$$\mathbf{w}_t \sim \mathcal{N}(\mathbf{0}, \mathbf{Q}) \quad (5.16)$$

$$\mathbf{v}_t \sim \mathcal{N}(\mathbf{0}, \mathbf{R}) \quad (5.17)$$

Since we assume that $\pi = p(\mathbf{x}_1)$ is also Gaussian, all our conditional probability distributions will be Gaussian due to the linearity of the transition and observation models. Once the parameters are obtained, the problem of inference and state estimation consists of

1. **Filtering.** We want to find $p(\mathbf{x}_t | \{\mathbf{y}_t\}_1^t)$. This is solved by the Kalman filtering algorithm.
2. **Smoothing.** We want to find $p(\mathbf{x}_t | \mathbf{Y})$. This is solved by the Kalman smoothing algorithm.
3. **Prediction.** We want to find $p(\mathbf{x}_{t+\tau} | \{\mathbf{y}_t\}_1^t)$. This is done by solving to 1. and then simulating using the state transition function.

We are mainly interested in filtering and smoothing.

Our problem

Although SSMs are well-suited for time-series data, they are not very well suited for our problem because the hidden state \mathbf{x}_t in this model is continuous, whereas in our problem, the sleeper's state is binary. While there are techniques to map from a continuous domain to a discrete one, we move on to discuss a more promising model.

5.6.3 Hidden Markov Models

Here, we present the Hidden Markov Models (HMMs), one of the most popular statistical models in machine learning with applications in many fields including but not limited to Cryptanalysis, Speech recognition and Bioinformatics [20]. The material presented here is based on [15], [16] and [7]. We will first present HMMs with discrete observations, then we extend this to include models with continuous observations.

Discrete observations

Similarly to SSMS, we have two sets of random variables. Observed variables $\mathbf{Y} = \{y_t\}_{t=1}^T$ which are drawn from the observation alphabet $V = \{v_1, \dots, v_M\}$, and hidden states $\mathbf{X} = \{x_t\}_{t=1}^T$ which are drawn from the hidden state alphabet $S = \{s_1, \dots, s_N\}$. The probabilistic graphical model of the HMM is identical to the one in Figure 5.4. The hidden states obey Markov assumptions, i.e. $P(x_t|x_{t-1}, \dots, x_1) = P(x_t|x_{t-1}) = \text{const.}, t = 2, \dots, T$. Moreover, the observed variables are only dependent on the corresponding hidden state, i.e. $P(y_t|x_t, \dots, x_1, y_{t-1}, \dots, y_1) = P(y_t|x_t), t = 1, \dots, T$.

We parameterise a HMM using the transition matrix \mathbf{A} , emission matrix \mathbf{B} , and the initial state distribution $\boldsymbol{\pi}$. The transition matrix $\mathbf{A} \in \mathbb{R}^{N \times N}$ describes the transitions between hidden states, $A_{ij} = P(x_{t+1} = s_j | x_t = s_i)$. The emission matrix $\mathbf{B} \in \mathbb{R}^{N \times M}$ describes the probability of an observation conditioned on a hidden state, $B_{jk} = B_j(v_k) = P(y_t = v_k | x_t = s_j)$. The initial state distribution $\boldsymbol{\pi} \in [0, 1]^N$ simply describes the initial probabilities of the hidden state, $\pi_i = P(x_1 = s_i)$. The model is fully described if we know these parameters, which we group into what is called a parameter set of the model, $\lambda = (\mathbf{A}, \mathbf{B}, \boldsymbol{\pi})$.

The three main questions of a HMM are

1. Find the probability of observations given the model, $P(\mathbf{Y}; \lambda)$.
2. Find the most likely series of hidden states \mathbf{X} to have generated the observations \mathbf{Y} , $\mathbf{X}^* = \arg \max_{\mathbf{X}} P(\mathbf{Y} | \mathbf{X}; \lambda)$.
3. Find the parameters λ to maximise $P(\mathbf{Y}; \lambda)$.

We will discuss algorithmic solution to these three problems in turn.

Solution to the first problem. To find the probability of an observed sequence, we use the dynamic programming algorithm, called the FORWARD PROCEDURE (outlined in Algorithm 1) which calculates the forward variable $\alpha_t(i) = P(\mathbf{Y}, x_t = s_i; \lambda)$. As we can see, the algorithm has a time complexity of $O(TN)$.

Algorithm 1 FORWARD PROCEDURE for computing $\alpha_t(i)$.

1. **Initialisation.**

$$\alpha_1(i) = \pi_i B_i(y_1), 1 \leq i \leq N$$

2. **Induction.**

$$\alpha_{t+1}(j) = \left[\sum_{i=1}^N \alpha_t(i) A_{ij} \right] B_j(y_{t+1}), \begin{matrix} 1 \leq t \leq T-1 \\ 1 \leq j \leq N \end{matrix}$$

3. **Termination.** (solution to the first problem)

$$P(\mathbf{Y}; \lambda) = \sum_{i=1}^N \alpha_T(i)$$

Solution to the second problem. To solve the problem of finding the most likely sequence of hidden states, we use the VITERBI ALGORITHM proposed by Andrew Viterbi in 1967. The most likely sequence of hidden states is also called the Viterbi path. Firstly, we define the quantity $\delta_t(i)$, which stores the highest probability along a single path ending at the state $x_t = s_i$:

$$\delta_t(i) = \max_{x_1, \dots, x_{t-1}} P(x_1, \dots, x_{t-1}, x_t = s_i, y_1, \dots, y_t; \lambda) \quad (5.18)$$

By induction, we have

$$\delta_{t+1}(j) = \left[\max_i \delta_t(i) A_{ij} \right] B_j(y_{t+1}) \quad (5.19)$$

We also keep track of the index of the hidden state that maximises this quantity in

$$\psi_{t+1}(j) = \arg \max_i \delta_t(i) A_{ij} \quad (5.20)$$

Having defined these quantities, we present the VITERBI ALGORITHM in Algorithm 2. As we can see, the algorithm has a time complexity of $O(TN^2)$.

Solution to the third problem. To learn the parameters of the model, $\lambda = (\mathbf{A}, \mathbf{B}, \boldsymbol{\pi})$, we use the FORWARD-BACKWARD ALGORITHM by Baum-Welch. We will need to introduce few quantities. Firstly, we introduce the backward variable $\beta_t(i) = P(y_{t+1}, \dots, y_T | x_t = s_i; \lambda)$ which can be computed using a dynamic programming algorithm in Algorithm 3. We also define the variable $\gamma_t(i) = P(x_t = s_i | \mathbf{Y}; \lambda)$

Algorithm 2 VITERBI ALGORITHM for computing the most likely sequence of hidden states.

1. **Initialisation.**

$$\begin{aligned}\delta_1(i) &= \pi_i B_i(y_1), & 1 \leq i \leq N \\ \psi_1(i) &= 0, & 1 \leq i \leq N\end{aligned}$$

2. **Recursion.**

$$\begin{aligned}\delta_t(j) &= \max_{1 \leq i \leq N} [\delta_{t-1}(i) A_{ij}] B_j(y_t), & 2 \leq t \leq T \\ & & 1 \leq j \leq N \\ \psi_t(j) &= \arg \max_{1 \leq i \leq N} [\delta_{t-1}(i) A_{ij}], & 2 \leq t \leq T \\ & & 1 \leq j \leq N\end{aligned}$$

3. **Termination.**

$$\begin{aligned}P^* &= \max_{1 \leq i \leq N} \delta_T(i) \\ x_T^* &= \arg \max_{1 \leq i \leq N} \delta_T(i)\end{aligned}$$

4. **Path backtracking.**

$$x_t^* = \psi_{t+1}(x_{t+1}^*), T-1 \geq t \geq 1$$

5. **Return** $\{x_t^*\}_1^T$.

Algorithm 3 BACKWARD ALGORITHM for computing $\beta_t(i)$.

1. **Initialisation.**

$$\beta_T(i) = 1, 1 \leq i \leq N$$

2. **Induction.**

$$\beta_t(i) = \sum_{j=1}^N A_{ij} B_j(y_{t+1}) \beta_{t+1}(j), \quad \begin{matrix} T-1 \leq t \leq 1 \\ 1 \leq j \leq N \end{matrix}$$

which can be expressed as

$$\begin{aligned}
\gamma_t(i) &= P(x_t = s_i | \mathbf{Y}; \lambda) \\
&= \frac{P(x_t = s_i, \{y_\tau\}_1^t; \lambda) P(\{y_\tau\}_{t+1}^T | x_t = s_i; \lambda)}{P(\mathbf{Y}; \lambda)} \\
&= \frac{\alpha_t(i) \beta_t(i)}{\sum_{i=1}^N \alpha_t(i) \beta_t(i)}
\end{aligned} \tag{5.21}$$

We also define the quantity $\xi_t(i, j)$ as

$$\begin{aligned}
\xi_t(i, j) &= P(x_t = s_i, x_{t+1} = s_j | \mathbf{Y}; \lambda) \\
&= \frac{\alpha_t(i) A_{ij} B_j(y_{t+1}) \beta_{t+1}(j)}{\sum_{i,j=1}^N \alpha_t(i) A_{ij} B_j(y_{t+1}) \beta_{t+1}(j)}
\end{aligned} \tag{5.22}$$

Now, we are in a position to present the FORWARD-BACKWARD ALGORITHM by Baum-Welch in Algorithm 4. The algorithm belongs to a family of Expectation-maximisation (EM) algorithms for finding maximum likelihood (ML) or maximum a posteriori (MAP) estimates of parameters in statistical models [19].

Algorithm 4 FORWARD-BACKWARD ALGORITHM (BAUM-WELCH) for estimating HMM parameters λ .

1. **Initialisation.** Set \mathbf{A} , \mathbf{B} , $\boldsymbol{\pi}$ to be random valid probability matrices/vectors.
2. **Repeat until convergence:**
 - **E-step.** Run FORWARD and BACKWARD PROCEDURES to get $\alpha_t(i)$ and $\beta_t(i)$. Evaluate $\gamma_t(i)$ using (5.21).
 - **M-step.** Re-estimate parameters using

$$\begin{aligned}
\pi_i &= \gamma_1(i) \\
A_{ij} &= \frac{\sum_{t=1}^{T-1} \xi_t(i, j)}{\sum_{t=1}^T \gamma_t(i)} \\
B_j(v_k) &= \frac{\sum_{t=1, \text{s.t. } y_t=v_k}^T \gamma_t(j)}{\sum_{t=1}^T \gamma_t(j)}
\end{aligned}$$

Parameters estimation with known hidden states. In case the hidden states \mathbf{X} are given to us, in addition to the observed variables \mathbf{Y} , the problem of parameters estimation simply reduces to counting

transitions, i.e.

$$A_{ij} = \frac{\sum_{t=1}^{T-1} 1\{x_t = s_i \wedge x_{t+1} = s_j\}}{\sum_{t=1}^T 1\{x_t = s_i\}} \quad (5.23)$$

$$B_j(k) = \frac{\sum_{t=1}^T 1\{x_t = s_j \wedge y_t = v_k\}}{\sum_{t=1}^T 1\{x_t = s_j\}} \quad (5.24)$$

where $1(\cdot)$ is an indicator function (1 if the boolean argument is true, 0 otherwise).

Continuous observations

We now discuss the case in which the observations $\mathbf{Y} = \{y_t\}_1^T$ are not drawn from a finite set V , but are real-valued vectors $\{\mathbf{y}_t\}_1^T$, drawn from \mathbb{R}^d , i.e. $\mathbf{y}_t \in \mathbb{R}^d, 1 \leq t \leq T$ (Note: hidden states $\mathbf{X} = \{x_t\}_1^T$ are still drawn from a finite set S). In this case, we cannot describe the observations using an emission matrix anymore. Since the observation random variables are now continuous, they must be drawn from some probability distribution function (pdf). This function can be any arbitrary pdf, however in order to learn anything useful, we parameterise it. We assume a simple case and let it be a Gaussian, parameterised by its mean, and covariance. In particular, $B_j(\cdot)$ becomes a probability distribution function:

$$\begin{aligned} B_j(\mathbf{y}_t) &= P(\mathbf{y}_t | x_t = s_j) \\ &= \mathcal{N}(\mathbf{y}_t; \boldsymbol{\mu}_j, \mathbf{U}_j), \end{aligned} \quad \begin{aligned} &1 \leq t \leq T \\ &1 \leq j \leq N \end{aligned} \quad (5.25)$$

This means that instead of the original emission matrix \mathbf{B} , we are now parameterising the emissions using the means $\boldsymbol{\mu} = \{\boldsymbol{\mu}_j \in \mathbb{R}^d\}_1^N$ and the covariances $\mathbf{U} = \{\mathbf{U}_j \in \mathbb{R}^{d \times d}\}_1^N$. Thus, our parameters set becomes $\lambda = \{\mathbf{A}, \boldsymbol{\mu}, \mathbf{U}, \boldsymbol{\pi}\}$.

Changes to the algorithms. While the three main questions for the HMM remain the same, we must change the algorithms used in the discrete observations case. It turns out that in the FORWARD PROCEDURE (Algorithm 1), BACKWARD PROCEDURE (Algorithm 3), and the VITERBI ALGORITHM (Algorithm 2), we don't need to change anything except the interpretation of $B_j(\cdot)$. Whereas before, we had a single value for this quantity, now we must evaluate it using the parameters of the pdf (in this case mean and covariance) in (5.25). The problem of estimating parameters, given the observations becomes slightly different and will be left untouched in our report. However, we discuss parameters estimation, given both

the observations and the hidden states, which simply becomes fitting a Gaussian, i.e.

$$\boldsymbol{\mu}_j = \frac{\sum_{t=1}^T 1\{x_t = s_j\} \mathbf{y}_t}{\sum_{t=1}^T 1\{x_t = s_j\}} \quad (5.26)$$

$$\mathbf{U}_j = \frac{\sum_{t=1}^T 1\{x_t = s_j\} (\mathbf{y}_t - \boldsymbol{\mu}_j)(\mathbf{y}_t - \boldsymbol{\mu}_j)^T}{\sum_{t=1}^T 1\{x_t = s_j\}} \quad (5.27)$$

Different probability density functions. We have assumed that the conditional distribution of the observations is Gaussian. One disadvantage of this method is that it may be too simple to capture the real pdf the observations are drawn from. One of the alternatives is the Gaussian Mixture Model (GMM), however fine-tuning the number of modes can be difficult. It turns out that finding the optimal MLE for a GMM is intractable [7].

Our problem

In our problem, we model the apnoeatic states as the hidden states $\{x_t\}_1^T$ drawn from a binary set $\{0, 1\}$. Although the observed signal is a sampled one-dimensional signal, since we only have annotations every K samples, we stack all K samples to a vector and treat it as a K -dimensional, real-valued observed variable $\mathbf{y}_t \in \mathbb{R}^d$, ($d = K$). Since we assume that we have the annotated signal, we can do the training offline. Thus we are interested in the third problem (with known hidden states), for which the solution is just fitting the parameters; and the second problem, finding the most likely sequence of the apnoeatic diagnoses, given the model and the observations, using the VITERBI ALGORITHM. We will train the model using the annotated data and once trained, we will use the trained model to diagnose sleep apnoea from new data. Implementations of the algorithms for our applications are available for MATLAB[®] in the packages pmtk3 (<https://github.com/probml/pmtk3>) and HMM Toolbox (<http://www.cs.ubc.ca/~murphyk/Software/HMM/hmm.html>) from Kevin Murphy.

5.6.4 Conditioning input data

Working in the time domain, the data is usually transformed to the frequency domain to analyse where the pattern is found more easily. Also, regardless of the chosen model, we will work in high dimensions which means we need a lot of input data in order to find the pattern. In the case of SVMs, it will be high-dimensional training points $\{\mathbf{x}^{(i)}\}_1^m$; in the case of SSMs and HMMs, it will be the high-dimensional observed variables $\{\mathbf{y}_t\}_1^T$. We will present two ways to condition the input data, before analysing it using the learning algorithms above, namely frequency-domain analysis and Principal Components Analysis.

Frequency-domain analysis

Discrete Fourier Transform. Discrete Fourier Transform (DFT) is used to transform a finite list of equally spaced samples of a function into the list of coefficients of a finite combination of complex sinusoids [18]. It can be said to convert the sampled function from its original domain to the frequency domain [18]. The DFT, \mathcal{F} , can be defined to transform $\mathbf{x} = \{x_1, x_2, \dots, x_N\}$ to $\mathbf{X} = \{X_1, X_2, \dots, X_N\}$ as

$$X_k = \sum_{n=1}^N x_n \exp(-i2\pi kn/N), 1 \leq k \leq N \quad (5.28)$$

and can be performed using the Fast Fourier Transform (FFT) algorithm.

Power Spectral Density. It is common to take the Power Spectral Density (PSD) instead of the DFT in order to remove the imaginary components in the frequency domain. The PSD of a continuous signal $x(t)$ can be defined as

$$S_{xx}(f) = \lim_{T \rightarrow \infty} \frac{1}{T} |X(f)|^2 \quad (5.29)$$

where $X(f)$ is the Fourier transform (\mathcal{FT}) of $x(t)$ in the interval $-T/2 < t < T/2$ [3]. It can be shown that in the discrete case where $\mathbf{x} = \{x_1, x_2, \dots, x_N\}$, the PSD is obtained by

$$S_{xx}(k) = \lim_{T \rightarrow \infty} \frac{(\Delta t)^2}{T} |X_k|^2 \quad (5.30)$$

$$\approx \frac{(\Delta t)^2}{T} |X_k|^2 \quad (5.31)$$

where T is the actual recording time, N is number of samples and $1/\Delta t$ is the sampling frequency (note that $T = N(\Delta t)$) [22].

Spectrograms. To create a spectrogram of a signal $\mathbf{x} = \{x_1, x_2, \dots, x_N\} = \{x(\Delta t), x(2\Delta t), \dots, x(N\Delta t)\}$, we must choose a window size T_{window} and an offset T_{offset} . Then, we keep shifting the window by T_{offset} and each time, we transform and store the window's content (in time domain) to the frequency domain using the DFT. This way, we will have a frequency domain data of the size T_{window} every T_{offset} , which we will call $\mathbf{X}_1, \mathbf{X}_2, \dots, \mathbf{X}_\tau$. We usually represent this frequency domain data using colour intensities and plot them as τ columns of colour intensities with time on the horizontal axis and frequency on the vertical axis. Figure 5.5 illustrates the process of creating a spectrogram. However, it is common to find the PSDs instead of the DFTs of the sliding windows (the principle stays the same). Hence we will refer to

the process of creating the spectrogram with PSDs (instead of DFTs) of the sliding windows as *frequency analysis of the signal*.

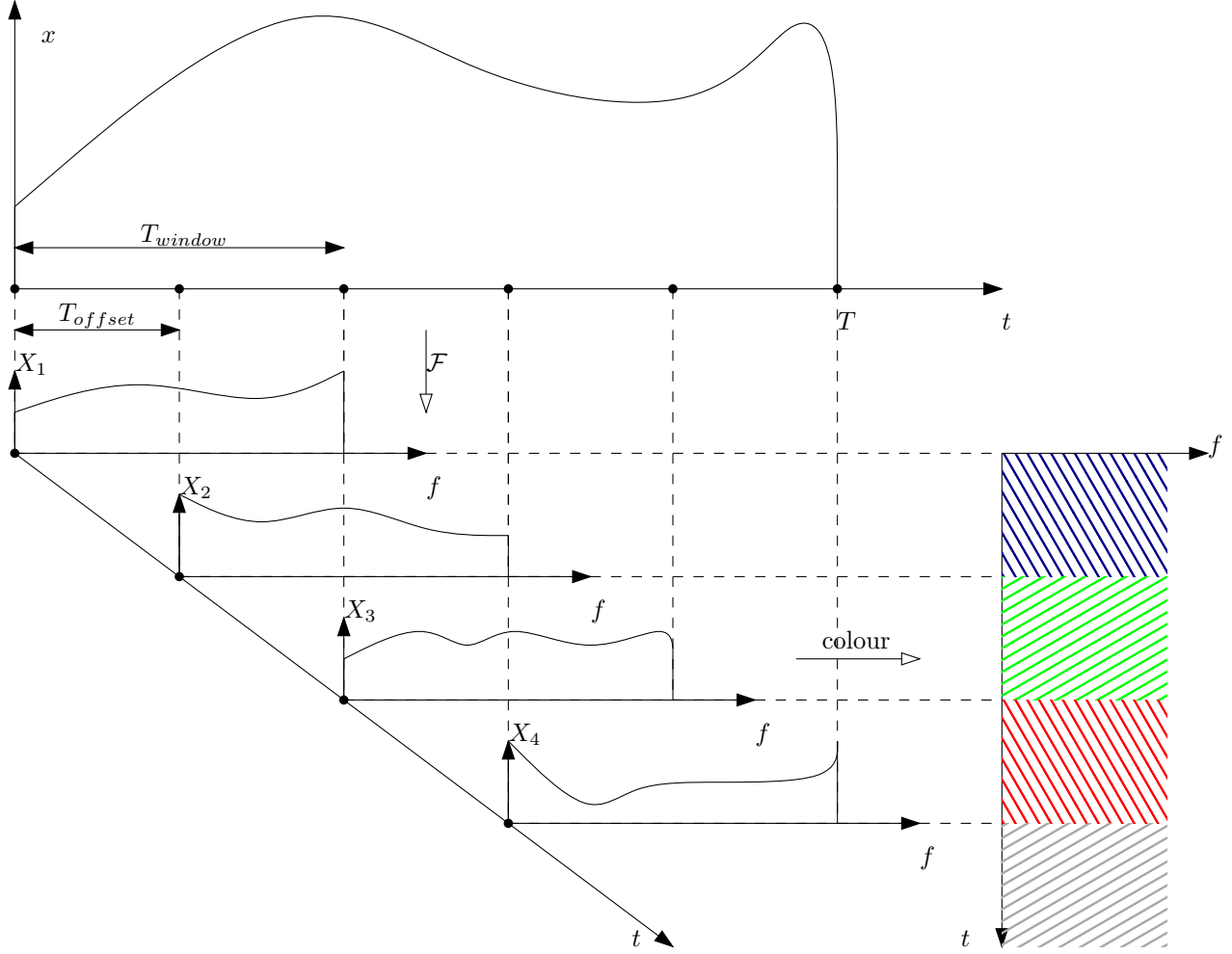


Figure 5.5: The process of creating a spectrogram.

Principal Components Analysis

Here we present the theory for Principal Components Analysis (PCA) based on Andrew Ng's lecture notes [8] and Kevin Murphy's book [7]. The objective is to take m n -dimensional input data points $\{\mathbf{x}^{(i)} \in \mathbb{R}^n\}_1^m$ and transform them into m k -dimensional data points ($k < n$) $\{\mathbf{y}^{(i)} \in \mathbb{R}^k\}_1^m$, where $\mathbf{y}^{(i)}$'s are projections of $\mathbf{x}^{(i)}$'s onto k orthonormal basis vectors $\{\mathbf{u}_i\}_1^k$ while "preserving the most variance". We assume that over all m points, their mean $\left[\{x_j^{(i)}\}_{i=1}^m\right] = 0$ and their var $\left[\{x_j^{(i)}\}_{i=1}^m\right] = 1$ for all features of the input points $1 \leq j \leq n$. We normalise the data first if this is not the case. For $n = 2$, $k = 1$, Figure 5.6 shows the projections to the new axis.

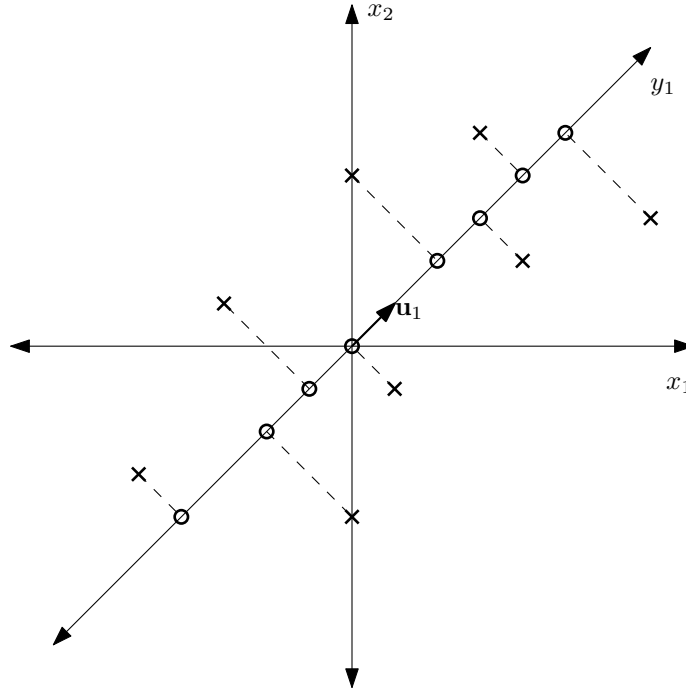


Figure 5.6: Illustration of PCA.

We can see that the transformed points can be expressed as

$$\mathbf{y}^{(i)} = \begin{bmatrix} \mathbf{u}_1^T \mathbf{x}^{(i)} \\ \mathbf{u}_2^T \mathbf{x}^{(i)} \\ \vdots \\ \mathbf{u}_k^T \mathbf{x}^{(i)} \end{bmatrix}, 1 \leq i \leq m \quad (5.32)$$

It can be shown that in order to maximise $\sum_{i=1}^m \|\mathbf{y}^{(i)}\|^2$, conditioned on orthonormality of the bases, we must choose normalised eigenvectors corresponding to the k largest eigenvalues of the variance matrix $\mathbf{\Sigma} = \frac{1}{m} \sum_{i=1}^m \mathbf{x}^{(i)} \mathbf{x}^{(i)T}$ as the bases. These bases are also called the *principal components*. The eigenvalues are proportional to the actual variances of data in the new bases. Hence, we can compare the relative “importance” of the bases and use this fact to decide how many principal components to use.

5.7 Machine Learning – Experiments

We obtained the data from the ECG database from the PhysioNet database located at <http://physionet.org/physiobank/database/apnea-ecg/>. The data consists of 35 labelled training records and 35 unlabelled records (used for the CinC Challenge 2000 competition). The recordings vary from less than 7 hours to 10 hours each and include continuous digitised ECG signal and, in the case of the training data, a set of apnoea annotations derived by human experts. The continuous signal is sampled at the rate of 100 Hz and the annotations are available at every 6000 samples (i.e. every minute) of the signal indicating the presence of apnoea at that time. One such record is shown in Figure 5.7.

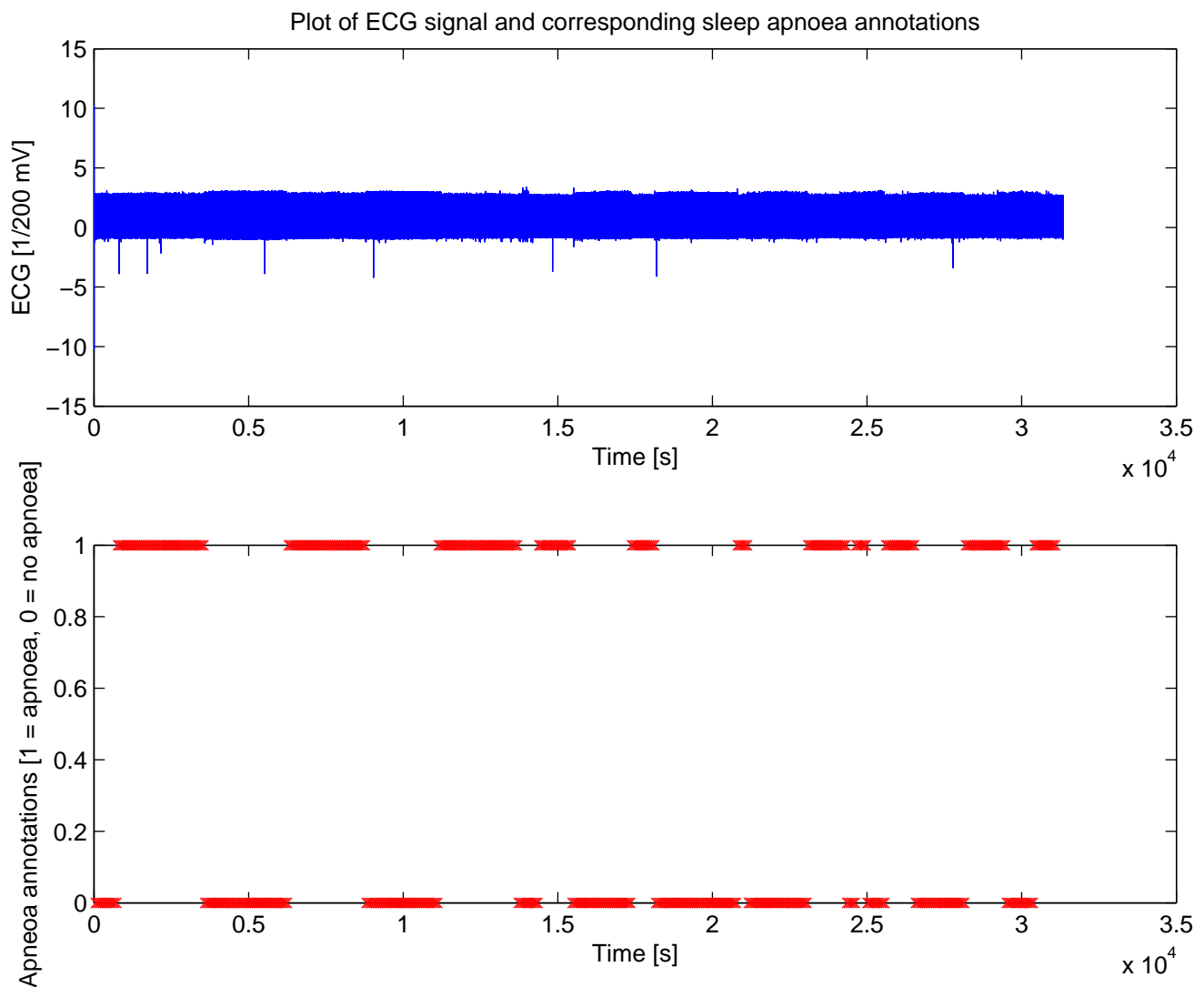


Figure 5.7: One training record

5.7.1 Conditioning input data

Frequency Analysis

We use MATLAB®’s function `spectrogram`, which takes the following parameters

- **X** – our signal $\mathbf{x} = \{x_1, x_2, \dots, x_N\}$.
- **WINDOW** – length (in number of samples) of the window T_{window} . The windows are automatically filtered using a Hamming window. We arbitrarily choose the window to be the number of signal samples corresponding to one annotation (6000 in our case).
- **NOVERLAP** – number of overlapping samples between two consecutive windows. Effectively $T_{\text{window}} - T_{\text{offset}}$. We arbitrarily choose the offset to be 1000 such that we have six bins of PSD’s for each annotation.
- **NFFT** – number of frequency points used to calculate the discrete Fourier transforms. We use default.
- **Fs** – sampling frequency in Hz. In our case 100 Hz.

A spectrogram for one record can be seen in Figure 5.8. Just by looking at the spectrogram, we can spot different regimes of the time series (most clearly seen at 0.5×10^4 , 1×10^4 , 2×10^4 , and 2.7×10^4 seconds). Comparing this to the apnoea annotations in Figure 5.7, these regimes are actually the non-apnoeatic regimes. Also, we can see that most of the “action” is happening below 20 Hz. For this reason, we cut off the frequencies above 25 Hz for subsequent analysis. We combine the corresponding six bins of PSD’s per annotation in to a large feature vector corresponding to that annotation. Next, we will reduce the dimensionality of these feature vectors using PCA.

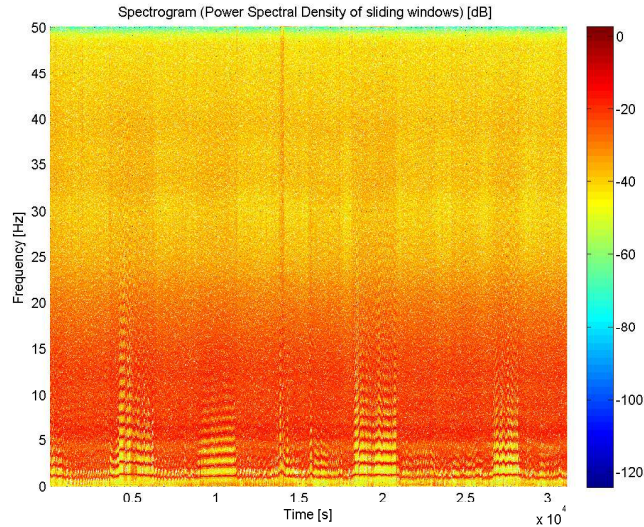


Figure 5.8: Spectrogram of one record

PCA

For this, we use the function `pca` from the package `pmtk3`. Once we get the principal components (orthogonal bases) and their corresponding principal coefficients (variances of the data, projected onto that base, correct to a constant factor) $\{\lambda_1, \lambda_2, \dots, \lambda_D\}$, we will plot the graph of their cumulative sum over their total sum $\frac{\sum_{i=1}^n \lambda_i}{\sum_{j=1}^N \lambda_j}$ in order to decide on the number of principal components needed. The plot is in the Figure 5.9. Performed on the first 10 records, we can see that we will need to include at least 100 to capture half of the variance but at least 3000 components to capture the whole variance.

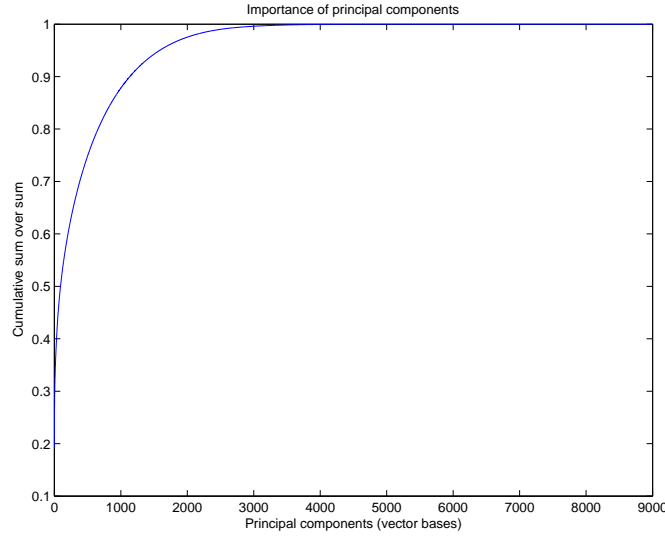


Figure 5.9: PCA of the first 10 records

5.7.2 Data Visualisation

It is helpful to visualise our data to confirm the presence of any detectable patterns and/or to help improve our learning algorithms. Since our Principal Component Analysis revealed that we need at least 100 principal components to capture at least half of the variance, it is not illustrative to visualise our data by plotting the data points on a 2D plane using only the first two principal components. Instead, we take the six corresponding bins of spectrograms of the two classes of annotations (apnoea, no apnoea) and take the average for each class as shown in Figure 5.10. We can notice the differences in the spectrograms which is reassuring because we can see that there exist some patterns to be found and that the spectrogram contains enough information to detect sleep apnoea.

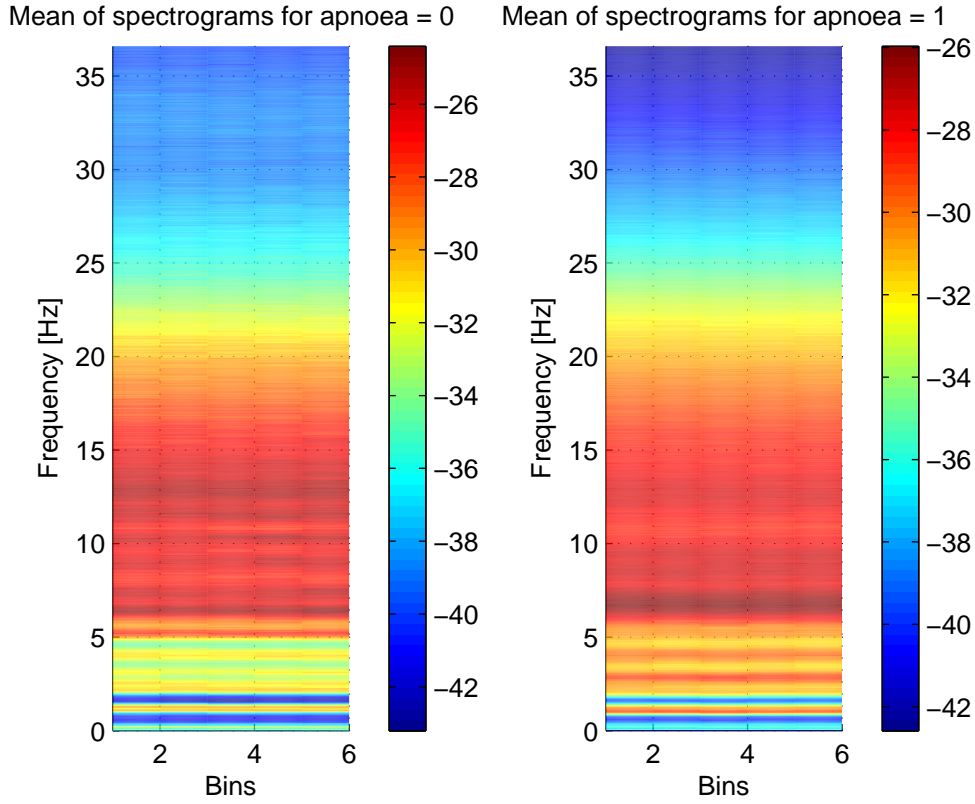


Figure 5.10: Comparison of the spectrograms of the two classes based on their average spectrogram from the first five records.

5.7.3 Support Vector Machines

Firstly, we investigate the case when no kernels are used. Then we will investigate the use of two possible kernels – polynomial (degree 3) and radial basis function. We will train on the first ten records using the MATLAB[®]’s function `svmtrain`. Then we will test our trained parameters on the next five records, where we record the accuracy as the ratio of the number of correctly classified annotations over the total number of annotations. We will also record the number of Support Vectors (SVs) because they indicate the generalisation performance.

No kernels

The results of this experiment are shown in Figure 5.11 and in Table 5.1. The accuracy is high, however so is the number of SV’s. This indicates that the generalisation guarantee is poor.

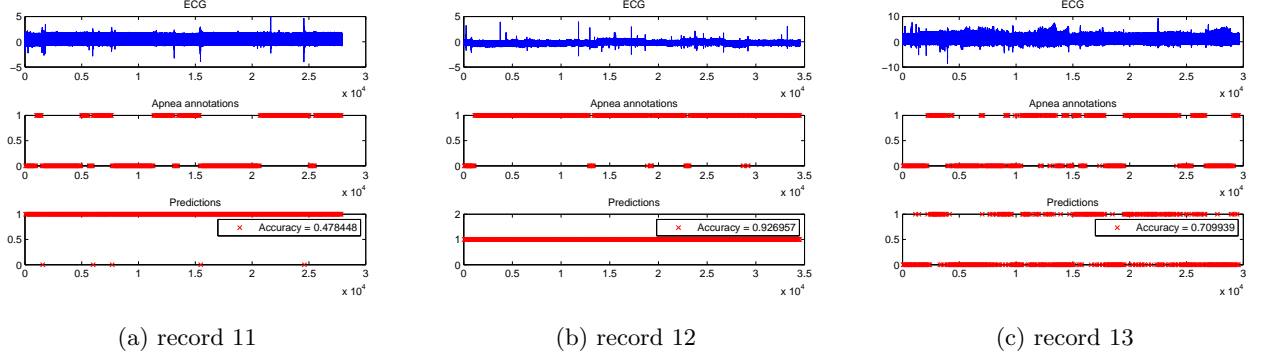


Figure 5.11: Performance of no kernels on the test records 11 to 15

Polynomial kernel

The results of this experiment are shown in Figure 5.12 and in Table 5.1. We can see that there is a low number of SVs and high accuracy. This means that the polynomial kernel is likely to perform well on unseen data. If we had more computational resources, we could have used more features (and correspondingly more training data) in order to represent the features better.

Radial basis function kernel

The results of this experiment are shown in Figure 5.13 and in Table 5.1. Similarly to the case of no kernels, the accuracy is high, but so is the number of SV's indicating poor generalisation performance.

Summary

Summary of the performances of the different kernels is shown in Table 5.1. The polynomial kernel with degree 3 is the most promising in terms of generalisation. All three kernels have similar accuracy. If we had more computational resources, we could have done deeper analysis and tests, e.g. use more principal components to capture as much variance as possible and use more training data (we only used 10 out of

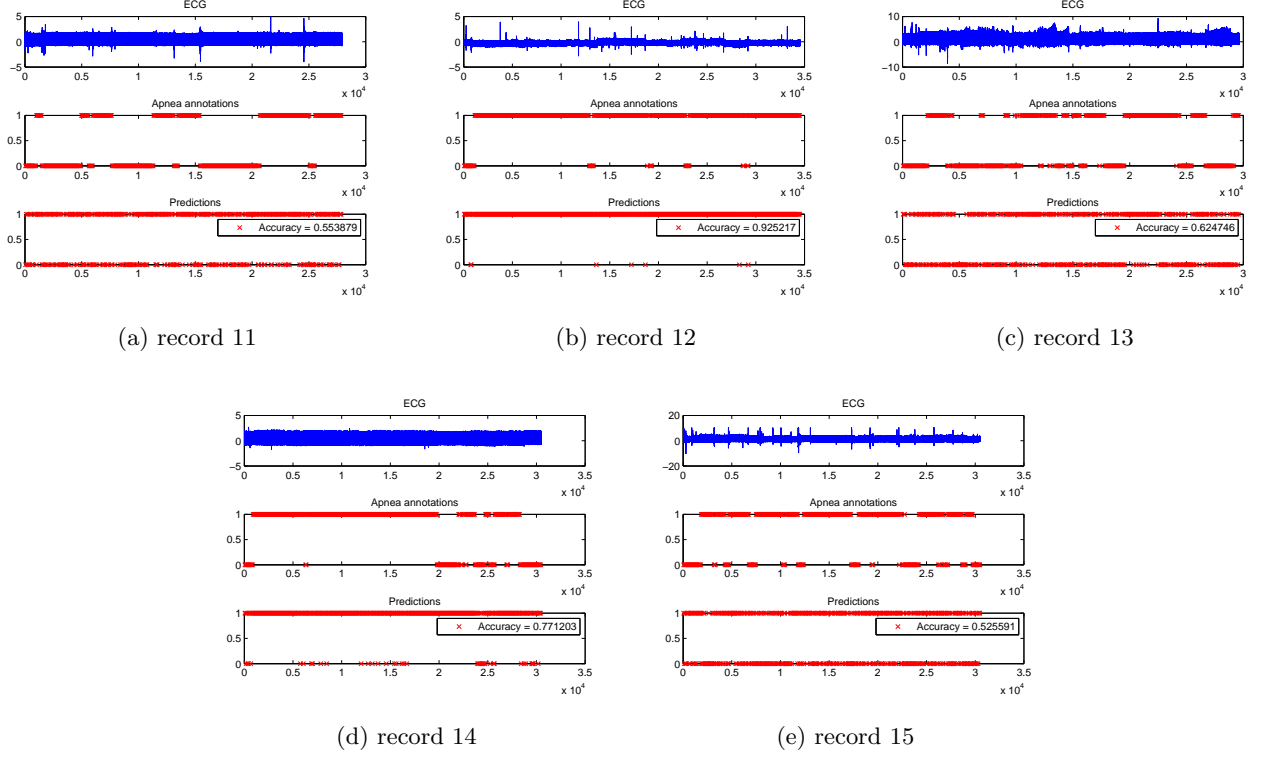


Figure 5.12: Performance of the polynomial kernel on the test records 11 to 15

35).

	# SV's (5005 data points)	Average accuracy
No kernel	3679	0.7116
Poly kernel	1879	0.6801
Rbf kernel	4033	0.6814

Table 5.1: Summary of performances of different kernels

5.7.4 Hidden Markov Models

Having examined briefly the theory behind Hidden Markov Models, let us now look at how the training was done offline, and analyse some results from subsequent tests. As mentioned earlier, the apnoeatic states are modelled as the hidden states $\{x_t\}_1^T$, and are elements of the binary set $\{0, 1\}$. The observed signal is annotated every K samples (every minute in the case of the PhysioNet data), so we stack all K samples into $\mathbf{y}_t \in \mathbb{R}^d$, ($d = K$). Using the packages `pmtk3` and `HMM Toolbox`, the algorithms were implemented in `MATLAB`[®], along with the conditioning of the data using spectrogram and PCA analysis. Again, `MATLAB`[®] is used for convenience and the code can be easily converted to `Java` after experimentation and analysis.

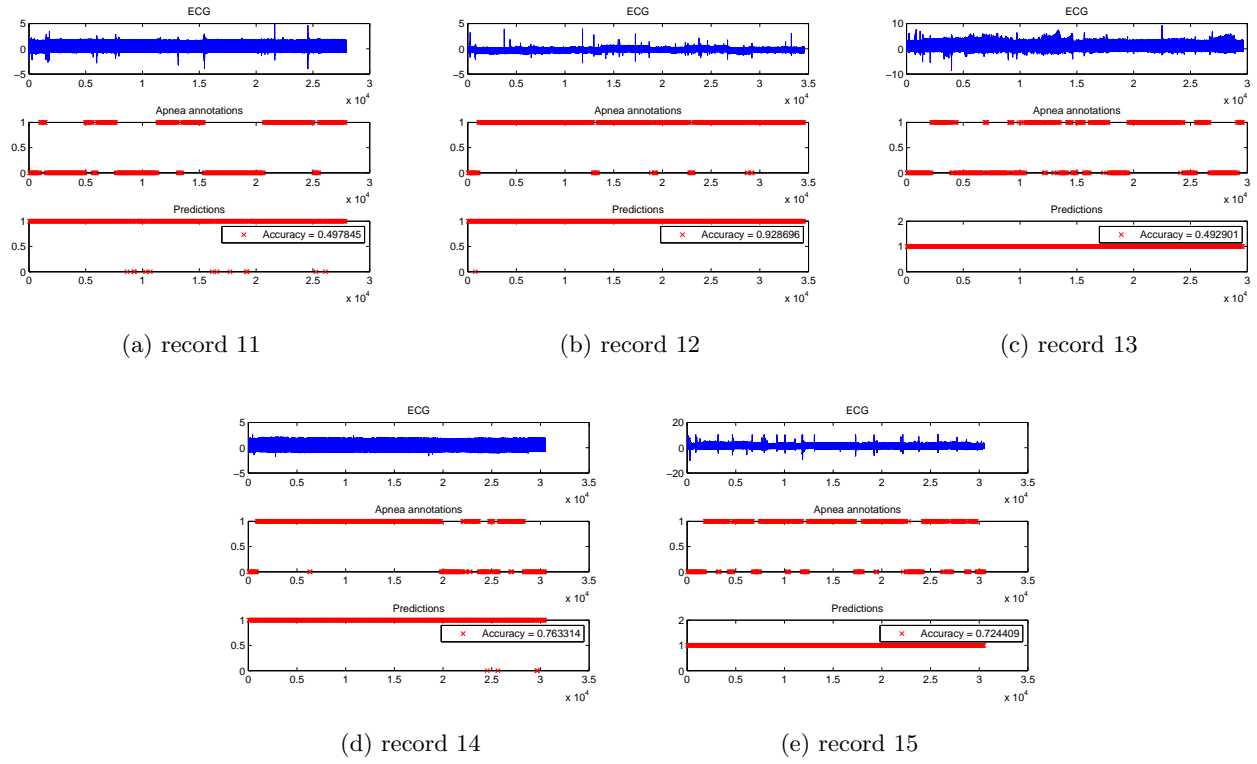


Figure 5.13: Performance of the Radial Basis Function kernel on the test records 11 to 15

We present below parts of the code used for the training and testing of the data, for ease of explanation. Firstly, we present the main script, covering the reading and conditioning of data, spectrogram transformation and PCA analysis. After explaining the various functions created and used in the script till then, we move on to cover the training and testing of the data.

```

1 trainIndex = 1:10;
2 testIndex = 11:15;
3
4 %% Reading and conditioning data
5 [Y, X] = readData(trainIndex, 0); % Y = observations, X = latent states.
6 N = 2; % number of states: apnea-noapnea
7 S = [0; 1]; % set of possible states
8
9 %% Transform spectrogram
10 [YTransformed, XTransformed] = transformSpectrogram(Y, X);
11
12 %% PCA

```

```

13 disp('PCA...');
14 k = 100; % take k principal components only
15 [PCoef, PVec, YMean, YVar] = pcaCalc(YTransformed, k);
16 figure;
17 plot(cumsum(PCoef)/sum(PCoef));
18 YPca = pcaTransform(YTransformed, PVec, YMean, YVar);

```

The trainIndex and testIndex vector are used simply for selecting the files to be used, out of 35, for training and the remainder (or less) for testing the accuracy of the diagnosis. Having chosen the files, the next step is to extract and read the files. This is done using the readData function, presented below:

```

1 function [O, q, time, signal, annTime] = readData(fileIndex, keepSignal)
2
3     disp('Reading and conditioning data...');
4     filenames = getFilenames();
5
6     % Initialise Variables (not shown)
7
8     for i = fileIndex
9         filename = cell2mat(filenames(i));
10        disp(sprintf('\tProcessing file %d: %s...', i, filename));
11
12        [timeTemp, signalTemp, freq] = rdsamp(filename); % reads the signal
13        [annTimeTemp, type] = rdann(filename, 'apn'); % reads annotations
14        type = (type == 'A');
15
16        %% Conditioning data
17        annTimeTemp = [1; annTimeTemp];
18        q = [q; type]; % latent states
19        for i = 1:length(type)
20            O = [O; signalTemp((annTimeTemp(i) + 1):annTimeTemp(i + 1))'];
21        end
22    end
23 end

```

The function reads data from the indices specified in fileIndex (which is trainIndex in the main script above), and returns O, containing all the observations merged together in a TxD matrix. T is the total

number of minutes of data, and D is the number of samples in a minute (6000 in this case), such that there are T annotations in total. The function also returns the vector q, a Tx1 vector containing the latent states for every minute in O, as well as consolidated time, signal and annotation time vectors for ease of plotting and analysis later on.

Firstly, readData uses a simple function getFilenames to return a 35x1 cell of the available filenames, in a cell string. Then, after initialising the variables, readData uses a for-loop to run through each file and extract the relevant information. Using the pre-provided rdsamp and rdann functions, the signal values as well as annotations are read from the file. As the annotations use 'A' for apnoeatic episodes and 'N' for non-apnoeatic episodes, the vector type is converted to the alphabet 0,1. The O and q output matrices are built up using the information from each file, and finally some trivial conditioning is done to ensure ease of plotting if the signal were to be kept.

Armed with the consolidated vectors X and Y, we now proceed to use the spectrogram function in MATLAB[®], as described in section 5.7.1. We then use the pca function from the pmtk3 package to perform Principal Components Analysis (choosing the number of principal components we wish to include, k).

We then move on to training and fitting the parameters, using the pmtk3 and HMM Toolbox packages. We then compare the expected hidden states calculated using the Viterbi Algorithm with the actual underlying states and determine the accuracy of the HMM model diagnosis.

```

1 %% Fitting parameters
2 [A, Mu, U, pi] = apneaHMM4Train(XTransformed, YPca, N, S);
3
4 %% Comparing with test data
5 apneaHMM7Test(A, Mu, U, pi, PVec, YMean, YVar, N, testIndex);

```

The parameters are fitted using the apneaHMM4Train function shown below (the number 4 simply represents the final version that we used), which computes the transitional matrix A using

$$A_{ij} = \frac{\sum_{t=1}^{T-1} 1\{x_t = s_i \wedge x_{t+1} = s_j\}}{\sum_{t=1}^T 1\{x_t = s_i\}} \quad (5.33)$$

and uses Gaussian fitting to calculate the pdfs for the emissions (the gaussFit function is used from the HMM Toolbox package - we shall not go into the details on how the function is implemented here). We are left with the outputs A, the 2x2 transition matrix, Mu and U, parameters of the Gaussian pdf fit of

the emissions, and π , the initial state distribution.

```
1 function [A, Mu, U, pi] = apneaHMM4Train(q, O, N, S)
2     [T, D] = size(O); % dimension of observations & number observations
3
4     % Transitional matrix A
5     disp('Fitting transitions...');
6     A = zeros(N);
7     for i = 1:N
8         for j = 1:N
9             transitionsFromSiToSj = 0;
10            transitionsFromSi = 0;
11            for t = 1:(T - 1)
12                transitionsFromSiToSj = transitionsFromSiToSj + (q(t) == S(i) && q(t ...
13                    + 1) == S(j));
14                transitionsFromSi = transitionsFromSi + (q(t) == S(i));
15            end
16            A(i, j) = transitionsFromSiToSj / transitionsFromSi;
17        end
18
19    % Estimate Gaussian parameters
20    disp('Fitting emissions...');
21    Mu = zeros(D, N); % means
22    U = zeros(D, D, N); % covariances
23    for j = 1:N
24        x = O(q == S(j), :);
25        model = gaussFit(x);
26        Mu(:, j) = model.mu;
27        U(:, :, j) = model.Sigma;
28    end
29
30    % Estimate HMM parameters
31    pi = [0.5; 0.5];
32 end
```

In order to compare with the test data, we need to read the data specified using the testIndex,

condition it, and use the **Viterbi Algorithm** to calculate the most likely path. This is done in the function `apneaHMM7Test`, shown below. The code for reading and conditioning the data (and plotting the results) has been omitted as it is similar to that shown above. Once again, functions from 'off-the-shelf' packages are used in implementing the **Viterbi Algorithm** and the accuracy of the most likely path is calculated by comparing it to the annotations reflecting the true states. This is done for each test file, and the results are shown below.

```

1 function apneaHMM7Test(A, Mu, U, pi, PVec, OMean, OVar, N, testIndex)
2     disp('Comparing with test data...');
3     accuracySum = 0;
4     for i = testIndex
5         %% Read data
6         %% Transform spectrogram
7         %% PCA
8
9         %% Most likely path (Viterbi)
10        disp(sprintf('\tCalculating the most likely path...'));
11        B = [];
12        for j = 1:N
13            B(j, :) = gaussian_prob(OTest', Mu(:, j), U(:, :, j));
14        end
15        path = viterbi_path(pi, A, B) - 1;
16
17        accuracy = sum(path == qTest') / length(qTest)
18        accuracySum = accuracySum + accuracy;
19
20        %% Plotting data
21    end
22    avgAccuracy = accuracySum / length(testIndex)
23 end

```

The results for the HMM experiment are shown in Figure 5.14. While the average accuracy is much lower than that found for the SVM model, at 64.1%, we feel that the HMM model would still be more appropriate than the SVM one due to the absence of Support Vectors which tend to lead to poor generalisation performance. Due to limited time and computational power (fitting the parameters takes a

considerable amount of time on a standard laptop), we were unable to utilise the full set of data for our experiments. However, we are confident that if more time and effort were to be expended in this area, the HMM model would prove to be more accurate in diagnosing apnoea as compared to the SVM model. This is because of the suitability of the Hidden Markov Model for temporal data and the applicability of the Markov assumptions in our case.

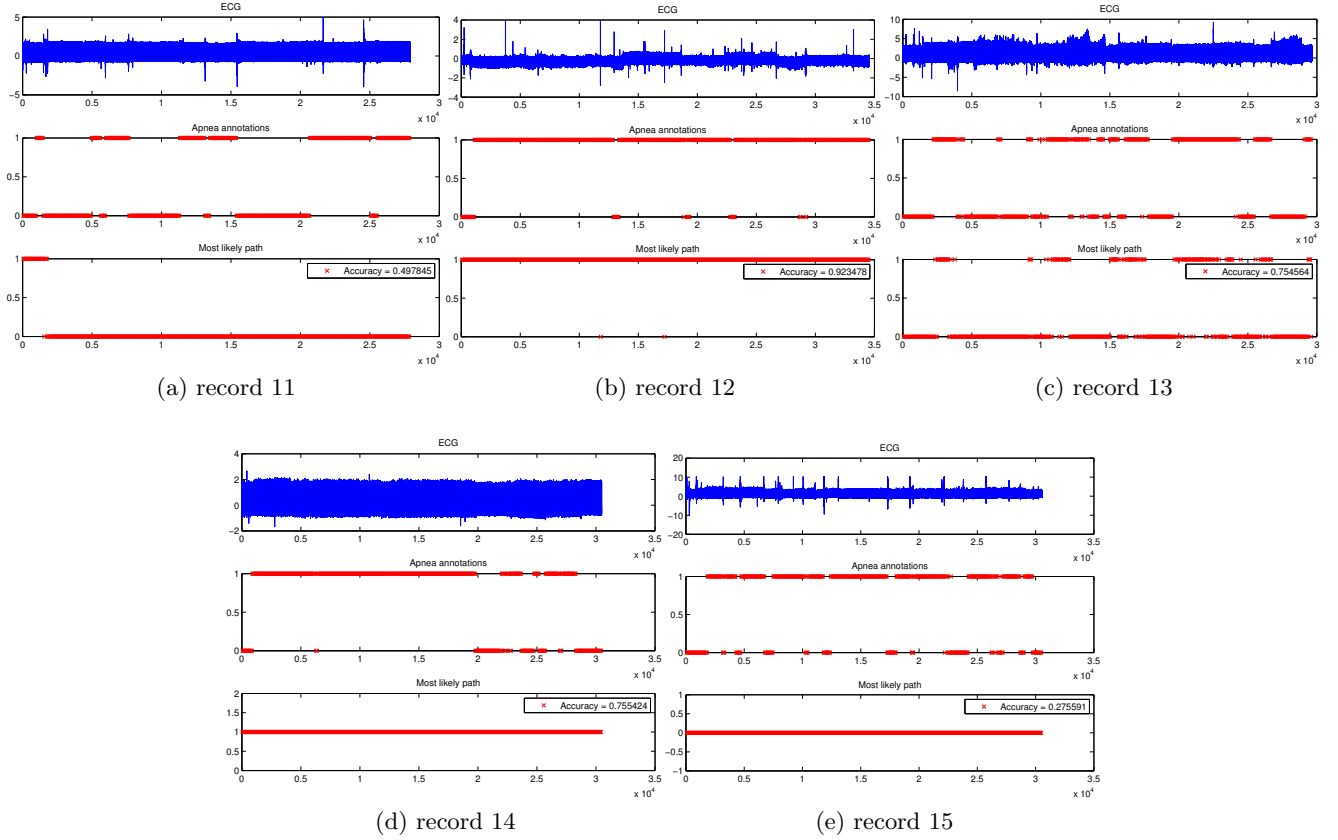


Figure 5.14: Performance of HMM model on the test records 11 to 15

5.7.5 Summary

We have seen the implementation of the SVM and HMM models to the PhysioNet data and have calculated the accuracy of both methods in diagnosing apnoea from five records. On the surface, while it may seem that the SVM model provides us with higher accuracy, we feel that the HMM model is more appropriate for use in our app. The accuracy can be improved, firstly, by using more data (we only used 10 of the 35 files for testing) and secondly, by ensuring that the annotations on training and testing data reflect the reality of the patient.

What we have managed to prove here, however, is that diagnosis of OSA using non-invasive techniques

is possible if the appropriate machine learning tools are utilised. If more resources were to be invested, an accurate and comprehensive diagnosis can be created in conjunction with the questionnaire.

5.8 Machine Learning – Java

5.9 Android

Chapter 6

Conclusion

Lorem ipsum dolor sit amet, consectetur adipisicing elit, sed do eiusmod tempor incididunt ut labore et dolore magna aliqua. Ut enim ad minim veniam, quis nostrud exercitation ullamco laboris nisi ut aliquip ex ea commodo consequat. Duis aute irure dolor in reprehenderit in voluptate velit esse cillum dolore eu fugiat nulla pariatur. Excepteur sint occaecat cupidatat non proident, sunt in culpa qui officia deserunt mollit anim id est laborum.

Bibliography

- [1] eMarketer.com. Smartphone users worldwide will total 1.75 billion, January 2014.
- [2] Zoubin Ghahramani and Geoffrey E Hinton. Variational learning for switching state-space models. *Neural computation*, 12(4):831–864, 2000.
- [3] A.M. Howatson, P.G. Lund, J.D. Todd, P.D. McFadden, P.J.P. Smith, and University of Oxford. Department of Engineering Science. *Engineering Tables and Data*. University of Oxford, Department of Engineering Science, 2008.
- [4] Wall Street Journal. A test for sleep apnea from your own bedroom, May 2013.
- [5] leahthegeek. Nick sleep apnea proof 1, 2007. Online Video - Accessed 8th January 2014.
- [6] MedIndia. Manipal university and xerox innovation to test remote-sensing healthcare technologies, February 2014.
- [7] Kevin P Murphy. *Machine learning: a probabilistic perspective*. Cambridge, MA, 2012.
- [8] Andrew Ng. Cs229 - lecture notes. Course website, 2013.
- [9] NHS. Sleep apnoea - diagnosis, June 2012.
- [10] NHS. Sleep apnoea, June 2014.
- [11] Novasom. Economics of home sleep testing, 2014.
- [12] Novasom. Why accusom?, 2014.
- [13] NPR. Apps for apnea? new gadgets promise to improve sleep, February 2012.
- [14] David Knott Steve Van Kuiken Peter Groves, Basel Kayyali. The 'big data' revolution in health care. *McKinsey & Company*, 2013.

- [15] Lawrence Rabiner. A tutorial on hidden markov models and selected applications in speech recognition. *Proceedings of the IEEE*, 77(2):257–286, 1989.
- [16] Daniel Ramage. Cs229 - section notes. Course website, 2007.
- [17] The Economic Times. Xerox, manipal to develop non-contact diagnostics solutions, February 2014.
- [18] Wikipedia. Discrete fourier transform — Wikipedia, the free encyclopedia, 2014. [Online; accessed 28-March-2014].
- [19] Wikipedia. Expectation-maximization algorithm — Wikipedia, the free encyclopedia, 2014. [Online; accessed 25-March-2014].
- [20] Wikipedia. Hidden markov model — Wikipedia, the free encyclopedia, 2014. [Online; accessed 24-March-2014].
- [21] Wikipedia. Machine learning — Wikipedia, the free encyclopedia, 2014. [Online; accessed 18-March-2014].
- [22] Wikipedia. Spectral density — Wikipedia, the free encyclopedia, 2014. [Online; accessed 14-April-2014].